Dynamics of interacting diseases

Joaquín Sanz,[1,2] Cheng-Yi Xia,[1,3] Sandro Meloni,[1] and Yamir Moreno[1,2,4]

[1]*Institute for Biocomputation and Physics of Complex Systems (BIFI), University of Zaragoza, Zaragoza 50018, Spain*
[2]*Department of Theoretical Physics, University of Zaragoza, Zaragoza 50009, Spain*
[3]*Key Laboratory of Computer Vision and System (Ministry of Education) and Tianjin Key Laboratory of Intelligence Computing and Novel Software Technology, Tianjin University of Technology, Tianjin 300191, P.R. China*
[4]*Complex Networks and Systems Lagrange Lab, Institute for Scientific Interchange, Turin, Italy*

Current modeling of infectious diseases allows for the study of complex and realistic scenarios that go from the population to the individual level of description. Most epidemic models however assume that the spreading process takes place on a single level (be it a single population, a meta-population system or a network of contacts). The latter is in part a consequence of our still limited knowledge about the interdependency of the many mechanisms and factors involved in disease spreading. In particular, interdependent contagion phenomena can only be addressed if we go beyond the scheme one pathogen-one network. In this paper, we study a model that allows describing the spreading dynamics of two concurrent diseases and apply it to a paradigmatic case of disease-disease interaction: the interaction between AIDS and Tuberculosis. Specifically, we characterize analytically the epidemic thresholds of the two diseases for different scenarios and also compute the temporal evolution characterizing the unfolding dynamics. Results show that there are regions of the parameter space in which the onset of a disease's outbreak is conditioned to the prevalence levels of the other disease. Moreover, we show that under certain circumstances, finite and not vanishing epidemic thresholds are found even at the thermodynamic limit for scale-free networks. Finally, we apply the formalism to qualitatively reproduce the incidence levels of the two persistent diseases that motivate our work.

PACS numbers:

arXiv:1402.4523v1 [physics.soc-ph] 18 Feb 2014

I. INTRODUCTION

The problem of how diseases spread has been studied since long time ago [1–8]. In the last few years, due to the increasing availability of data about transmission patterns, contact networks and population mobility, it has become apparent that we are in the position to develop theoretical and computational frameworks that will ultimately allow the forecast of epidemic outbreaks [9–26]. The latter is a consequence of the increasing availability of new models that are capable of providing better predictions of real epidemic scenarios [27]. In particular, we have been able to identify what ingredients are key to characterize the unfolding of a disease outbreak. This is the case of the structure of the population in the form of networks of contacts at a local scale [9, 17, 19, 28], or of individual mobility patterns that facilitate the spreading of diseases in wider geographical areas [29]. The theoretical implications of considering these aspects have been thoroughly addressed [30–33], and at the same time, the amount and quality of real data that are relevant to epidemic spreading is constantly increasing [34, 35].

In this context, an emergent field of research is the modeling of coupled spreading phenomena, whether they are two pathogens or multiple strains of the same disease that propagates concurrently on the same population [33, 36–39]. Focusing on the two-pathogen scenario, the complexity of the problem increases because now the natural history of one of the diseases is affected by the presence of the second one, typically as a consequence of the modification of the host's immune response after infection $-$ with a plethora of possibilities as given by different schemes of interactions $-$. In addition, the networks of contacts through which the pathogens spread can vary from one disease to the other. Typical examples of these coupled spreading phenomena are given by the interaction between HIV infection and the spreading of certain opportunist pathogens [40, 41], or the strain-strain interactions of a viral pathogen like the flu virus [43].

From a theoretical point of view, one of the first works that considered the above problem from a networked point of view is due to Funk and Jensen in 2010 [37]. In their work, the authors exploited the analogy of the spreading process with a bond-percolation problem so as to address the issue of epidemic thresholds in a SIR (Susceptible-Infected-Removed) model. However, this first work did not consider a framework in which the temporal evolution of the epidemics can be studied. More recently, Marceau et al. presented a new model [39] aimed at studying the latter aspect, also in a SIR model, using "on-the-fly graphs", a network generation model previously introduced by the authors [45]. Once again, although the temporal evolution of the system can be observed within their modeling approach, it does not provide any information about epidemic thresholds. In addition, the model can not be trivially generalized so as to cover other classical models like SIS (Susceptible-Infected-Susceptible).

In this work, we propose a modeling framework for the spreading of two concurrent diseases that allows to explicitly derive the epidemic threshold of each disease in terms of the parameters that characterize the evolution of both diseases and the topology of the networks of contacts. Moreover, we show that the approach here adopted naturally describes the temporal evolution of the system's dynamics and that it can be straightforwardly extended to other classical models for epidemic spreading (SIR, SIS, SEIR, etc). Finally, we also discuss several cases that might be relevant in real scenarios and show qualitatively how our approach could be used to study interacting diseases such as AIDS and Tuberculosis.

The rest of the paper is organized as follows. In the second section, we introduce the model. Then, we analytically derive the expressions for the epidemic thresholds, which are later compared to extensive numerical simulations in section four. Finally, we perform a finite size analysis to inspect the behavior of the model $-$more precisely, of the critical thresholds$-$ when approaching the thermodynamic limit.

II. THE MODEL

Our purpose in this work is to explore an epidemiological scenario in which two different infectious diseases simultaneously spread through the same host population, and whose dynamical parameters (i.e. infectiousnesses and recovery rates) depend, at the level of single individuals, on whether the agents involved have caught only one of the diseases or both. In addition, we consider that neither the mechanisms behind each disease evolution nor the contact networks through which they spread have to be the same, and thus, are considered independently for each disease.

Let us then consider that we have two diseases (disease 1 and disease 2) which spread over two different networks of contacts: disease 1 propagates over network 1, which has a mean degree $\langle k\rangle = \sum_{k,l} P(k,l)k$; whilst disease 2 does so over network 2, whose mean connectivity is equal to $\langle l\rangle = \sum_{k,l} P(k,l)l$. The composed degree distribution $P(k,l)$ gives the proportion of nodes (individuals) having k and l links in networks 1 and 2, respectively.

As a first step, we will consider the baseline scenario in which the isolated dynamics of each disease, when the second is absent, is described by a simple S-I-S scheme. So, each individual belonging to a composed connectivity classes (k,l) can be in four different dynamical states: susceptible with respect to both diseases $s(k,l)$, infected of both $\rho(k,l)$, and infected with the first (second) one and still susceptible to catch the second (first) disease, $\rho_1(k,l)$ ($\rho_2(k,l)$); being these quantities the proportion of individuals at each disease state belonging to the composed degree class (k,l). Thus, we have that $s(k,l) + \rho_1(k,l)+\rho_2(k,l)+\rho(k,l) = 1\ \forall(k,l)$. In addition, regardless of the connectivities of the nodes involved, we have eight possible contagion transitions after a contact (four for each disease). On the other hand, (fully or partially) recovered individuals are so

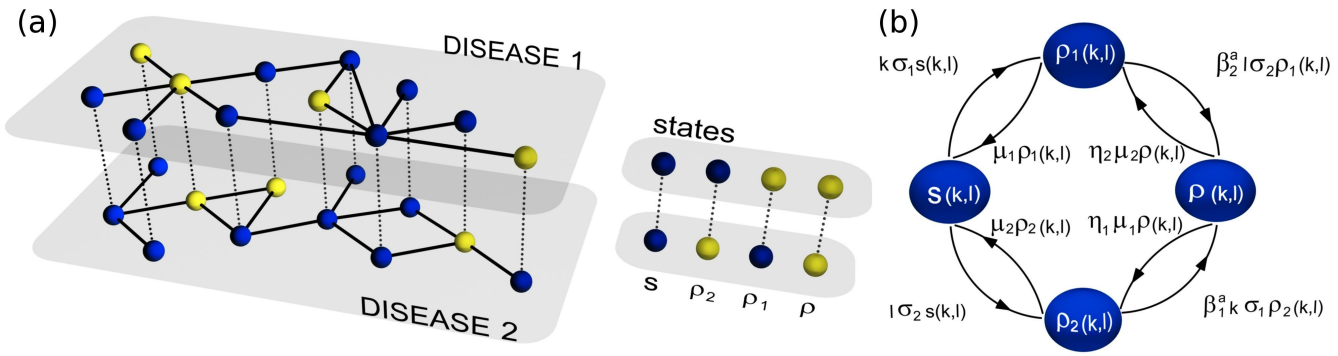

FIG. 1: (color online) (a) Each of the diseases spreads over a different network. Each individual belongs simultaneously to each network and can be *ornot* infected with each of the diseases. (b) Set of transitions allowed in the model. The variables $(s(k,l), \rho_1(k,l), \rho_2(k,l), \rho(k,l))$ represent the densities of individuals of each type in the system having k neighbors in network 1 and l neighbors in network 2.

after four possible transitions from an infected class. This amounts to a total of twelve elementary transitions, schematized as follows (see also Figure. 1):

$$
\begin{aligned}
\rho_1 + s &\xrightarrow{\lambda_1} \rho_1 + \rho_1 \\
\rho_1 + \rho_2 &\xrightarrow{\beta_1^a \lambda_1} \rho_1 + \rho \\
\rho + s &\xrightarrow{\beta_1^b \lambda_1} \rho + \rho_1 \\
\rho + \rho_2 &\xrightarrow{\beta_1^a \beta_1^b \lambda_1} \rho + \rho \\
\rho_2 + s &\xrightarrow{\lambda_2} \rho_2 + \rho_2 \\
\rho_2 + \rho_1 &\xrightarrow{\beta_2^a \lambda_2} \rho_2 + \rho \\
\rho + s &\xrightarrow{\beta_2^b \lambda_2} \rho + \rho_2 \\
\rho + \rho_1 &\xrightarrow{\beta_2^a \beta_2^b \lambda_2} \rho + \rho \\
\rho_1 &\xrightarrow{\mu_1} s \\
\rho_2 &\xrightarrow{\mu_2} s \\
\rho &\xrightarrow{\eta_1 \mu_1} \rho_2 \\
\rho &\xrightarrow{\eta_2 \mu_2} \rho_1
\end{aligned}
$$

The model thus contains two basic infection probabilities –λ_1 and λ_2– as well as two basic recovery rates –μ_1 and μ_2–, one for each disease. In addition, infection probabilities are affected by scaling factors –the four β parameters and combinations of them– and so are the recovery rates –by the η parameters–, as it is explained in detail in Table I. The introduction of these parameters describe the interaction of the diseases through three different effects that are concurrently taken into account. The first effect is the variation of the susceptibility of healthy individuals to get infected with one disease as a consequence of being infected with the other. This mechanism is described by β_1^a for the risk variation of infection of disease 1 caused by disease 2, and β_2^a, for the symmetric case. The second effect is the variation of the spreading capabilities of double-infected individuals with respect to single-infected ones, which is described by the parameters β_1^b and β_2^b, for diseases 1 and 2, respectively. The last effect is the variation of the infectious periods of double-infected individuals also with respect to single-infected ones, described by η_1 and η_2.

The introduction of these parameters exhaustively describes all the ways in which two diseases can interact according to a SIS scheme, and allows us to isolate the different effects of one disease on the spreading of the other by making infectious individuals more efficient spreaders or by making susceptible individuals more prone to get sick. Once we have defined the whole set of parameters in table I, we have all possible transitions between dynamical states well defined (see Figure 1). According to the scheme depicted in the figure (in which simultaneous double contagions and recoveries from both diseases have

Parameter	Dynamical meaning
λ_1	Baseline infectiousness of disease 1
λ_2	Baseline infectiousness of disease 2
μ_1	Baseline recovery rate of disease 1
μ_2	Baseline recovery rate of disease 2
β_1^a	Variation of disease 1 infectiousness due to the fact that the susceptible individual exposed to disease 1 is infected with disease 2
β_2^a	Variation of disease 2 infectiousness due to the fact that the susceptible individual exposed to disease 2 is infected with disease 1
β_1^b	Variation of disease 1 infectiousness due to the fact that the spreader is also infected with disease 2
β_2^b	Variation of disease 2 infectiousness due to the fact that the spreader is also infected with disease 1
η_1	Variation of disease 1 recovery rate for individuals also infected with disease 2
η_2	Variation of disease 2 recovery rate for individuals also infected with disease 1

TABLE I: Model parameters

$\theta_1^{\rho_1} = \frac{\sum_{k,l} P(k,l)k\rho_1(k,l)}{\sum_{k,l} P(k,l)k}$	probability of a given link of network 1 pointing to a ρ_1 node
$\theta_1^{\rho} = \frac{\sum_{k,l} P(k,l)k\rho(k,l)}{\sum_{k,l} P(k,l)k}$	probability of a given link of network 1 pointing to a ρ node
$\theta_2^{\rho_2} = \frac{\sum_{k,l} P(k,l)l\rho_2(k,l)}{\sum_{k,l} P(k,l)l}$	probability of a given link of network 2 pointing to a ρ_2 node
$\theta_2^{\rho} = \frac{\sum_{k,l} P(k,l)l\rho(k,l)}{\sum_{k,l} P(k,l)l}$	probability of a given link of network 2 pointing to a ρ node

TABLE II: Theta parameters

been explicitly excluded), the set of differential equations describing the evolution in time of the four densities of individuals $(s(k,l), \rho_1(k,l), \rho_2(k,l), \rho(k,l))$ is as follows:

$$\dot{s}(k,l) = -k\lambda_1\theta_1^{\rho_1}s(k,l) - l\lambda_2\theta_2^{\rho_2}s(k,l) - k\beta_1^b\lambda_1\theta_1^{\rho}s(k,l) - l\beta_2^b\lambda_2\theta_2^{\rho}s(k,l) + \mu_1\rho_1(k,l) + \mu_2\rho_2(k,l) \quad (1)$$

$$\dot{\rho_1}(k,l) = k\lambda_1\theta_1^{\rho_1}s(k,l) + k\beta_1^b\lambda_1\theta_1^{\rho}s(k,l) - l\beta_2^a\lambda_2\theta_2^{\rho_2}\rho_1(k,l) - l\beta_2^a\beta_2^b\lambda_2\theta_2^{\rho}\rho_1(k,l) - \mu_1\rho_1(k,l) + \eta_2\mu_2\rho(k,l) \quad (2)$$

$$\dot{\rho_2}(k,l) = l\lambda_2\theta_2^{\rho_2}s(k,l) + l\beta_2^b\lambda_2\theta_2^{\rho}s(k,l) - k\beta_1^a\lambda_1\theta_1^{\rho_1}\rho_2(k,l) - k\beta_1^a\beta_1^b\lambda_1\theta_1^{\rho}\rho_2(k,l) - \mu_2\rho_2(k,l) + \eta_1\mu_1\rho(k,l) \quad (3)$$

$$\dot{\rho}(k,l) = k\beta_1^a\lambda_1\theta_1^{\rho_1}\rho_2(k,l) + l\beta_2^a\lambda_2\theta_2^{\rho_2}\rho_1(k,l) + k\beta_1^a\beta_1^b\lambda_1\theta_1^{\rho}\rho_2(k,l) + l\beta_2^a\beta_2^b\lambda_2\theta_2^{\rho}\rho_1(k,l) - (\eta_1\mu_1 + \eta_2\mu_2)\rho(k,l) \quad (4)$$

where the θ parameters are defined in Table II.

Combining the probabilities θs and defining the following two new parameters $\sigma_1 = \lambda_1(\theta_1^{\rho_1} + \beta_1^b\theta_1^{\rho})$ and $\sigma_2 = \lambda_2(\theta_2^{\rho_2} + \beta_2^b\theta_2^{\rho})$ we obtain the average probabilities per link for s nodes to become infected with disease 1 (σ_1) or disease 2 (σ_2). This allows us to rewrite the system of differential equations as:

$$\dot{s}(k,l) = -(k\sigma_1 + l\sigma_2)s(k,l) + \mu_1\rho_1(k,l) + \mu_2\rho_2(k,l) \quad (5)$$

$$\dot{\rho_1}(k,l) = k\sigma_1 s(k,l) - l\beta_2^a\sigma_2\rho_1(k,l) - \mu_1\rho_1(k,l) + \eta_2\mu_2\rho(k,l) \quad (6)$$

$$\dot{\rho_2}(k,l) = l\sigma_2 s(k,l) - k\beta_1^a\sigma_1\rho_2(k,l) - \mu_2\rho_2(k,l) + \eta_1\mu_1\rho(k,l) \quad (7)$$

$$\dot{\rho}(k,l) = k\beta_1^a\sigma_1\rho_2(k,l) + l\beta_2^a\sigma_2\rho_1(k,l) - (\eta_1\mu_1 + \eta_2\mu_2)\rho(k,l) \quad (8)$$

Only three of these four equations are linearly independent for each composed connectivity class (k,l), due to the closure relationship $s(k,l) + \rho_1(k,l) + \rho_2(k,l) + \rho(k,l) = 1\ \forall(k,l)$. Taking this into account, we next analyze the time evolution of the vector $(\rho_1(k,l), \rho_2(k,l), \rho(k,l))$, since $s(k,l) = 1 - \rho_1(k,l) - \rho_2(k,l) - \rho(k,l)$.

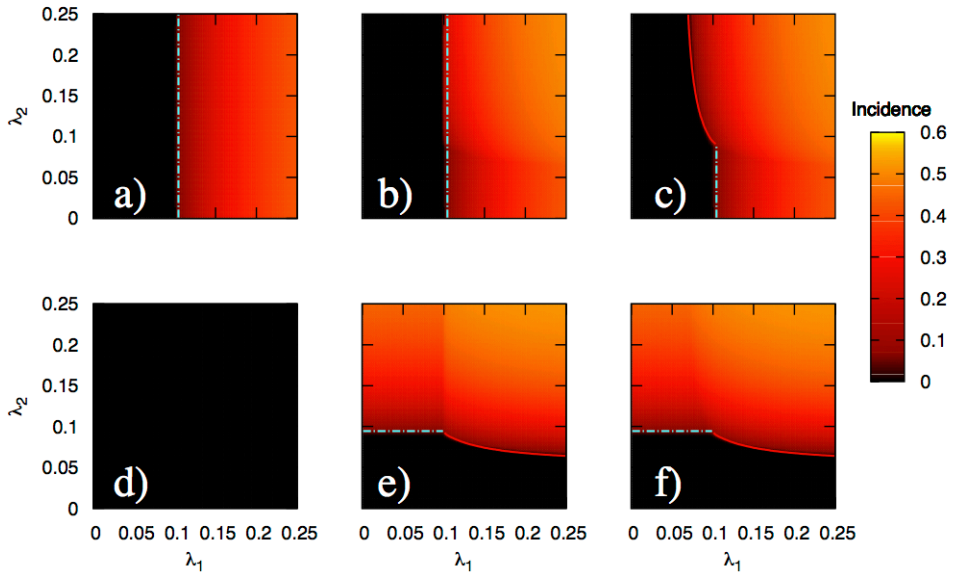

FIG. 2: (color online) Reciprocally enhanced spreading. Dynamical parameters: $\mu_1 = \mu_2 = 0.75$, $\beta_1^a = \beta_1^b = \beta_2^a = \beta_2^b = 1.3$, $\eta_1 = \eta_2 = 0.8$. Networks: Erdös-Renyi graphs: $N_1 = N_2 = 5000$ agents, $\langle k \rangle = 7$, $\langle l \rangle = 8$. The color maps represent the prevalence levels of diseases 1 – upper panels – and 2 – lower panels –, at different stages of the Monte-Carlo simulations. Step 1 (panels a,d): stationary levels after the initial introduction of an infection seed of disease 1 ($\epsilon_{\rho_1} = 0.005$). Step 2 (panels b,e): once stage 1 is completed, an infection seed of disease 2 ($\epsilon_{\rho_2} = 0.005$) is introduced, and stationarity is recovered. Step 3: (panels c,f): after stage 2, an additional seed of infection 1 is re-introduced ($\epsilon_{\rho_1} = 0.005$), and the stationary prevalences plotted. Dashed and solid lines represent respectively primary and secondary thresholds predicted by the model.

III. EPIDEMIC THRESHOLDS

In order to analyze the most relevant dynamical properties of the system, we look for the values $(\rho_1^*(k,l), \rho_2^*(k,l), \rho^*(k,l))$ that define the stationary state: $(\dot{\rho}_1^*(k,l), \dot{\rho}_2^*(k,l), \dot{\rho}^*(k,l)) = (0,0,0)\ \forall (k,l)$ for the system Eq. (8). In order to do that, we are forced to consider σ_1 and σ_2 as additional parameters, although these two quantities are linear combinations of the other variables and the ultimate responsible of the coupling among the variables of all connectivity classes. As it happens commonly in this kind of models [6, 17], there exists a trivial fixed point of the dynamics in which there are no infected individuals in the system: $(\rho_1^*(k,l), \rho_2^*(k,l), \rho^*(k,l)) = (0,0,0)\ \forall (k,l)$. This fixed point represents the absorbing state of our model. In addition, there are other possible fixed points for which the densities of infected individuals could be written as a function of the σ parameters: $(\rho_1^*(k,l,\sigma_1,\sigma_2), \rho_2^*(k,l,\sigma_1,\sigma_2), \rho^*(k,l,\sigma_1,\sigma_2)) \neq (0,0,0)$.

It is thus possible to get self-consistent equations for the variables σ as:

$$\sigma_1 = f_1(\sigma_1,\sigma_2) = \frac{\lambda_1}{\langle k \rangle} \sum_{k,l} P(k,l) k (\rho_1(k,l,\sigma_1,\sigma_2) + \beta_1^b \rho(k,l,\sigma_1,\sigma_2)) \tag{9}$$

$$\sigma_2 = f_2(\sigma_1,\sigma_2) = \frac{\lambda_2}{\langle l \rangle} \sum_{k,l} P(k,l) l (\rho_2(k,l,\sigma_1,\sigma_2) + \beta_2^b \rho(k,l,\sigma_1,\sigma_2)) \tag{10}$$

The condition $\sigma_1 = f_1(\sigma_1,\sigma_2) > 0$ implies the existence of a stable active state for the dynamics of disease 1, i.e., a state in which disease 1 becomes endemic in the population. For this situation to take place for disease 2, the condition $\sigma_2 = f_2(\sigma_1,\sigma_2) > 0$ must be fulfilled. Given the symmetry between the two expressions in Eq. (10), we will focus only on the analysis of the first equation. In fact, it can be showed that always $\frac{\partial^2 f(\sigma_1,\sigma_2)}{\partial \sigma_1^2} < 0$, which means that, if we think of the graphical solution of the equation $\sigma_1 = f_1(\sigma_1,\sigma_2)$, for this non trivial solution to exist –given that, obviously $f(\sigma_1 = 0, \sigma_2 = 0) = 0$– it

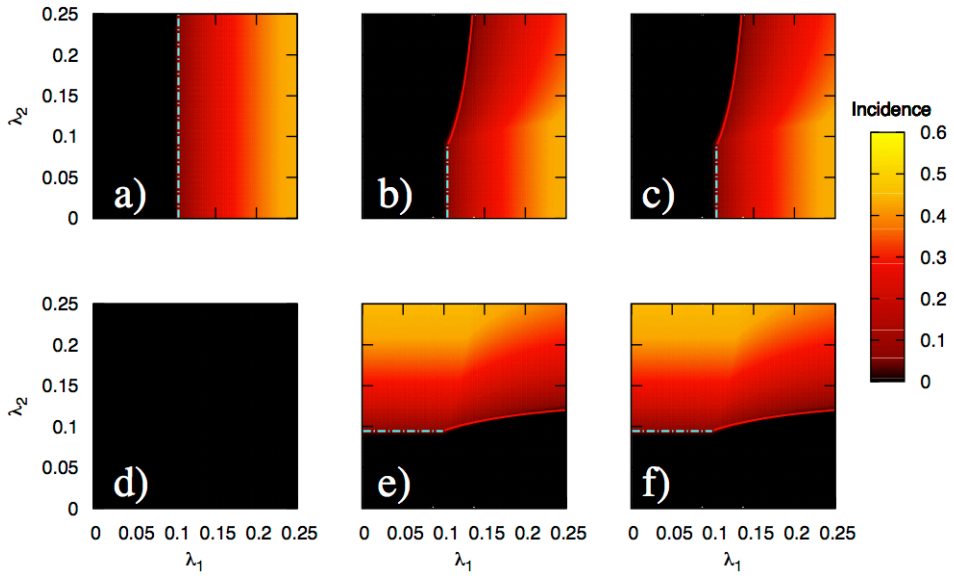

FIG. 3: (color online) Reciprocally impaired spreading. Dynamical parameters: $\mu_1 = \mu_2 = 0.75$, $\beta_1^a = \beta_1^b = \beta_2^a = \beta_2^b = 0.8$, $\eta_1 = \eta_2 = 1.3$. Networks: Erdös-Renyi graphs: $N_1 = N_2 = 5000$ agents, $\langle k \rangle = 7$, $\langle l \rangle = 8$. The color maps represent the prevalence levels of diseases 1 – upper panels – and 2 – lower panels –, at different stages of the Monte-Carlo simulations. As it is done in figure 2, we introduce successively three infectious seeds $(\rho_1, \rho_2, \rho_1) = 0.005$, and plot the stationary prevalences after each fluctuation in the three columns of the figure. As it can be seen, the reintroduction of the third seed of infection 1 in the system does not affect the prevalence levels, as global stability is reached after the second stage.

must be verified that $\left[\frac{\partial f(\sigma_1,\sigma_2)}{\partial \sigma_1}\right]_{\sigma_1=0} > 1$, as in [17]. After some algebra, this condition yields the following expression:

$$\frac{\lambda_1 \sum_{k,l} P(k,l) k^2 \frac{l^2\sigma_2^2\beta_2^a\beta_1^a\beta_1^b + l\sigma_2(\eta_2\mu_2\beta_1^a + \beta_1^b(\beta_1^a\mu_1 + \beta_2^a\mu_2)) + \mu_2(\eta_1\mu_1 + \eta_2\mu_2)}{l^2\sigma_2^2\beta_2^a\eta_1 + l\sigma_2(\eta_1\mu_1 + \eta_2\mu_2 + \beta_2^a\eta_1\mu_2) + \mu_2(\eta_1\mu_1 + \eta_2\mu_2)}}{\mu_1\langle k \rangle} > 1 \tag{11}$$

that allows us to derive the epidemic threshold as:

$$\lambda_1^c(\sigma_2) = \mu_1 \frac{\langle k \rangle}{\sum_{k,l} P(k,l) k^2 \frac{l^2\sigma_2^2\beta_2^a\beta_1^a\beta_1^b + l\sigma_2(\eta_2\mu_2\beta_1^a + \beta_1^b(\beta_1^a\mu_1 + \beta_2^a\mu_2)) + \mu_2(\eta_1\mu_1 + \eta_2\mu_2)}{l^2\sigma_2^2\beta_2^a\eta_1 + l\sigma_2(\eta_1\mu_1 + \eta_2\mu_2 + \beta_2^a\eta_1\mu_2) + \mu_2(\eta_1\mu_1 + \eta_2\mu_2)}} \tag{12}$$

Looking at the latter expression −which contains the underlying topologies in a more intricate way than for the uncoupled, classical case−, the threshold dependence on disease 2's prevalence via σ_2 becomes explicit. If we evaluate $\lambda_1^c(\sigma_2 = 0)$ we recover the classical result $\lambda_1^c = \mu_1\langle k \rangle / \langle k^2 \rangle$ [9, 17]. Therefore, in the following we will refer to this baseline case as primary threshold, $\lambda_1^c(0)$, whereas the more general case will be referred to as the secondary threshold, $\lambda_1^c(\sigma_2)$ (with $\sigma_2 > 0$). Obviously, the same stands for the primary $(\lambda_2^c(0))$ and secondary thresholds $(\lambda_2^c(\sigma_1))$ of the second disease.

A particular case for the topologies on top of which both diseases are spreading corresponds to the homogeneous mean field version of the system, i.e., $P(k,l) = \delta(k - k_o)\delta(l - l_o)$, for which the last expression can be rewritten as:

$$\lambda_1^c(\sigma_2) = \frac{\lambda_2 l_o}{k_o} \frac{\eta_1\mu_1(\beta_2^a(\lambda_2 l_o - \mu_2) + \mu_1) + \eta_2\mu_2\mu_1}{\mu_2(\eta_2\mu_2 + \eta_1\mu_1) + (\lambda_2 l_o - \mu_2)(\beta_2^a\beta_1^a\beta_1^b(\lambda_2 l_o - \mu_2) + \beta_1^a\beta_1^b\mu_1 + \eta_2\mu_2\beta_1^a + \beta_2^a\beta_1^b\mu_2)} \tag{13}$$

An independent derivation of this expression can be achieved after analyzing the Jacobian matrix of the homogeneous mean field system analogous to Eq. (8) as it is shown in the Appendix A.

IV. PHASE DIAGRAMS

In order to explore the quality of the threshold prediction of our model, we have designed a Monte-Carlo simulation scheme in which a single state transition is allowed per individual per time step. First, infected individuals will eventually spread the disease(s) that they carry. As double events are not allowed at a single time step, forbidden double transitions from s to ρ are solved choosing just one of the diseases for the individual to get infected with according to the status of their infected neighbors: the more neighbors one individual has carrying disease 1 rather than disease 2, the more likely he will become infected with disease 1 rather than with disease 2. After the spreading loop is complete for both diseases, infected nodes who have not suffered any contagion at the present time step eventually recovers from the diseases they carry. To avoid forbidden double recoveries from the ρ class to the s class, in those cases the only disease the individual is going to recover from is also chosen stochastically, according to the probabilities $p_1 = \eta_1\mu_1/(\eta_1\mu_1 + \eta_2\mu_2)$ for the first disease, and $p_2 = 1 - p_1$ for the second one.

Let us first explore a simple scenario in which we assume that the dynamical effects of one disease on the other are totally symmetric. In terms of the parameters of the model, this implies that $\beta_1^a = \beta_2^a = \beta_1^b = \beta_2^b \equiv \beta$ and $\eta_1 = \eta_2 \equiv \eta$. In this case, let's focus on two opposite scenarios: i) mutual enhancement: $\eta < 1$ and $\beta > 1$ and ii) (partial) cross immunity $\eta > 1$ and $\beta < 1$. In the case of mutual enhancement, individuals who are infected with the second disease, spread and become infected with disease 1 more easily than those who are not (this is because $\beta > 1$). In addition, since also $\eta < 1$, infected individuals of disease 1 remain so for longer times if they are also infected with the second disease. These two effects imply that the appearance of disease 2 in the system enhances the spreading capabilities of disease 1. The reciprocal situation is also true, as the interaction between both diseases is symmetric. Finally, in the case of partial cross immunity, the effects on the infectiousness and recovery rates are the opposite, and so the appearance of one of the diseases at a certain prevalence impairs the spreading of the other disease. In Figures 2–3, we represent the prevalence of each disease, as a function of the baseline infectiousnesses (λ_1, λ_2) for a given set of parameters after the introduction of infection seeds in a given order as shown. The networks through which diseases spread are, for this first case, two uncorrelated Erdös-Renyi graphs.

For the case of mutual enhancement, (figure 2), given our set of parameters, the analytically-obtained curves for the secondary threshold remain below the primary thresholds, yielding the appearance of two regions in the plane (λ_1, λ_2), for which it is verified $\lambda_1^c(\sigma_2) < \lambda_1 < \lambda_1^c(0)$ and $\lambda_2^c(\sigma_1) < \lambda_2 < \lambda_2^c(0)$, respectively. The dynamical relevance of these regions is that within them, the appearance of an outbreak of one of the diseases is conditional to the previous installation of the other infection in the system. In this way we can observe that, after an initial seed of ρ_1 individuals, disease 1 does not become endemic in the region $\lambda_1^c(\sigma_2) < \lambda_1 < \lambda_1^c(0)$ (fig. 2, panel a), but then, after the outbreak of the second disease in the network, the same seed leads disease 1 to become endemic in that same region (fig. 2 panel C) as predicted by our model. Regarding the conjugate region in which $\lambda_2^c(\sigma_1) < \lambda_2 < \lambda_2^c(0)$, we can see in figure 2, panel e, that disease 2 directly becomes endemic after the introduction of an infection seed ρ_2 due to the fact that, previously, disease 1 was already introduced in the system.

The situation for the partial cross immunity case is the opposite, and the secondary thresholds remain, in this case, above the primary ones. So, in this scenario, we have another couple of relevant regions in which $\lambda_1^c(0) < \lambda_1 < \lambda_1^c(\sigma_2)$ and $\lambda_2^c(0) < \lambda_2 < \lambda_2^c(\sigma_1)$, respectively. In figure 2, it is represented the behavior of the system under these conditions. In panel a, we can see how disease 1 becomes endemic after the introduction of an initial seed above its primary threshold. Then, after introducing a seed of disease 2, as shown in panel b for the area comprised between $\lambda_1^c(0)$ and $\lambda_1^c(\sigma_2)$, the prevalence of disease 1 vanishes. In other words, in that region, the introduction of disease 2 makes the system to recover from disease 1. If we look at the behavior of the second disease in the region in which $\lambda_2^c(0) < \lambda_2 < \lambda_2^c(\sigma_1)$, we see how the disease is unable to become endemic as a consequence of the fact that the first disease has already been introduced in the system. This situation suggests that, as it has already been addressed in the context of computational sciences [47], the introduction of an infectious agent designed to immunize its host with respect to another, more harmful infection, might be a conceptually feasible option to reduce the prevalence of the latter, or even to eradicate it. This has also been recently reported in the context of multi-strain diseases, in which more than one strain of the same disease compete for the host population [33].

Once the model dynamics has been exhaustively characterized when the diseases spread over homogeneous networks, we move on and explore the influence of degree heterogeneity on the dynamics. To this end we also perform intensive numerical simulations in an analogous way, but using scale free graphs of the same size as before with different exponents. In Figure 4 we represent the final prevalence for each disease in two configurations: reciprocally enhanced diseases −panels a and c− and impaired spreading −panels b and d−. In both cases, network 1 ($\gamma = 2.7$, panels a and b) has a greater power law exponent than network 2 ($\gamma = 2.5$, panels c and d). As it can be seen, for both diseases and for both configurations, secondary thresholds are closer to primary ones than in the case of homogeneous networks.

V. SYSTEM SIZES AND EPIDEMIC THRESHOLDS: GENERAL CASE

In the previous sections we have described the baseline cases in which none of the dynamical parameters vanishes, and both networks are, in each case, of the same kind –Erdos-Renyi or uncorrelated scale-free graphs–. A relevant question yet remains unanswered, i.e., how the epidemic thresholds behave when the system size grows and eventually reaches the thermodynamic

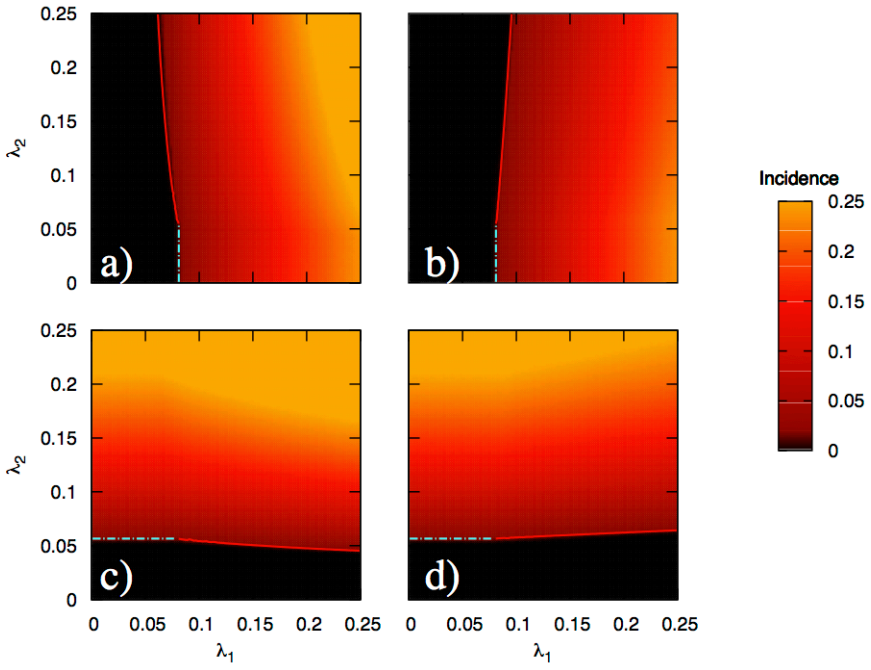

FIG. 4: (color online) Panels a and c: reciprocally enhanced spreading with $\beta_1^a = \beta_1^b = \beta_2^a = \beta_2^b = 1.3$, $\eta_1 = \eta_2 = 0.8$, represented at the final stationary state. Panels b and d: reciprocally impaired spreading $\beta_1^a = \beta_1^b = \beta_2^a = \beta_2^b = 0.8$, $\eta_1 = \eta_2 = 1.3$, also at the final state. Scale-free networks are generated using the uncorrelated configuration model with $N_1 = N_2 = 5000$ agents, $\langle k \rangle = 4.00$, and $\langle l \rangle = 5.11$. The figure represents the final prevalence of diseases 1 (panels a and b) and 2 (panels c and d) in each case.

limit. Regarding this question, we present an exhaustive analysis in Appendix B, in which it is shown what are the conditions that lead to have vanishing small secondary thresholds as a function of the underlying topologies and some of the dynamical parameters. The results show that the secondary epidemic threshold associated to any of the diseases that is spreading over a scale-free network with $2 < \gamma \leq 3$ vanished at the thermodynamic limit, regardless of the topology of the network on top of which its conjugate disease propagates and of the values of the dynamical parameters. In an analogously robust way, power laws with $\gamma > 3$ −or homogeneous degree distributions− yield finite, non vanishing secondary thresholds at the thermodynamical limit, regardless of the conjugate topologies or parameter values, with some exceptions.

The relevance of this result relies on the fact that the model predicts the same behavior for the epidemic thresholds in heterogeneous and homogeneous networks as compared with classical models of uncoupled (single) diseases that spread over simple networks. In addition, our analysis shows that the eventual vanishing of the epidemic thresholds for infinite systems is only determined by the topology of the network under consideration rather than by any possible coupling with another disease that spreads over any other possible conjugate network within our model framework. However, there is an exception to this general behavior which is meaningful from an epidemiologically viewpoint. This is the case when both diseases spread over two highly and positively correlated scale-free networks with composed degree distribution $P(k,l) = \delta(k-l)\alpha k^{-\gamma}$, where δ stands for the Kronecker δ-function and α is a normalization constant. In that situation, if we focus, for example, in disease 1, there exist two different interaction schemes of interest for which we recover finite epidemic thresholds $\lambda_1^c > 0$ at the thermodynamic limit even for scale-free graphs with $2 < \gamma \leq 3$:

- Scheme 1: Individuals infected with disease 2 become immune to infection by disease 1. $\beta_1^a = 0$; $(\beta_2^a, \beta_2^b, \beta_2^b)$ are free parameters.
- Scheme 2: Even being $\beta_1^a \neq 0$, individuals infected with both diseases can not cause contagion of disease 1: $\beta_1^b = 0$. In addition, disease 1 can not cause total immunity to disease 2: $\beta_2^a \neq 0$. β_2^b is a free parameter.

To illustrate this situation, we take as an example a particular case of the first scheme, a mutual cross-immunity scenario given by $\beta_1^a = \beta_2^a = 0$. In order to point out the role of inter-layer degree correlations on this effect, we can directly compare the expression for the threshold when both networks are totally correlated with the analogous expression derived from a uncorrelated combined degree distribution:

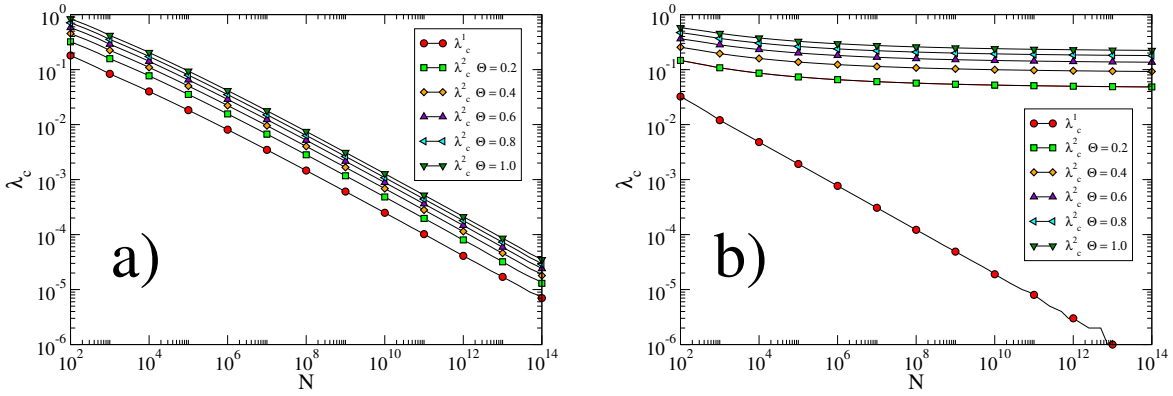

FIG. 5: (color online) Primary and Secondary threshold values as a function of the size of the systems N for different values of Θ: 0.0 (primary threshold), 0.2, 0.4, 0.6, 0.8 and 1.0. Networks are uncorrelated scale free graphs (panel a) without correlations between them –panel a– or with them –panel b, fully correlated–. Diseases interact according to a full cross-immunity scheme $\beta_a^1 = \beta_a^2 = 0$ and $\gamma = \Gamma = 2.5$. The rest of the parameters are the same as in figure 2.

$$P(k,l) = \delta(k-l)\alpha k^{-\gamma} \rightarrow \lambda_1^c(\sigma_2) = \mu_1 \frac{\langle k \rangle}{\sum_k \alpha \frac{1}{k^{2-\gamma}} \frac{\mu_2}{k\sigma_2+\mu_2}} \tag{14}$$

$$P(k,l) = \alpha k^{-\gamma} l^{-\Gamma} \rightarrow \lambda_1^c(\sigma_2) = \mu_1 \frac{\langle k \rangle}{\sum_{k,l} \alpha \frac{1}{k^{2-\gamma}} \frac{1}{l^{\Gamma}} \frac{\mu_2}{l\sigma_2+\mu_2}} \tag{15}$$

In Figure 5, we represent the values predicted by these expressions for different network sizes, when $\gamma = \Gamma = 2.5$. As we can see in panel a, for uncorrelated networks, regardless of the value of σ_2, the threshold continuously decreases as we increase network sizes. The result thus shows that the existence of a coupling with another disease present in the system with a certain prevalence proportional to σ_2, does not play any role, since the heterogeneities in the degrees still constitute the main reason leading to the vanishing of the threshold at the thermodynamical limit. This picture turns out to be remarkably different when we introduce positive, strong correlations between the two networks. In that case, as we can see in panel b, the appearance of the second disease, characterized by a certain prevalence level $\sigma_2 > 0$, implies a sudden change in the behavior of the threshold, that does not vanish anymore, even when $N \rightarrow \infty$.

The influence of degree correlations between networks for this case of full cross-immunity becomes evident also at finite sizes, since the differences between primary and secondary thresholds, as seen in figure 6, is also greatly amplified. Another eventually relevant effect that can be observed in the last figure is that the transition that takes place at the epidemic threshold is much sharper in the case of correlated networks. All the previous results point out that the worst scenario for the spreading of a disease when it interacts with a second one that confers immunity to the former corresponds to the case in which there is a correlation between heterogeneous networks of contacts. This finding is essentially equivalent to what was found previously in [37], what we have shown here is that the effect comes to revert the vanishing threshold at the thermodynamic limit for disease spreading on top of scale-free networks. In addition, we have found that it is not needed for this effect to take place that the second disease confers full immunity to disease one.

VI. DISCUSSION AND CONCLUSIONS

In this work, we propose a composed mean field model to describe the simultaneous spreading of two diseases over the same population but driven by independent mechanisms of transmission taking place on different networks of contacts. Within this

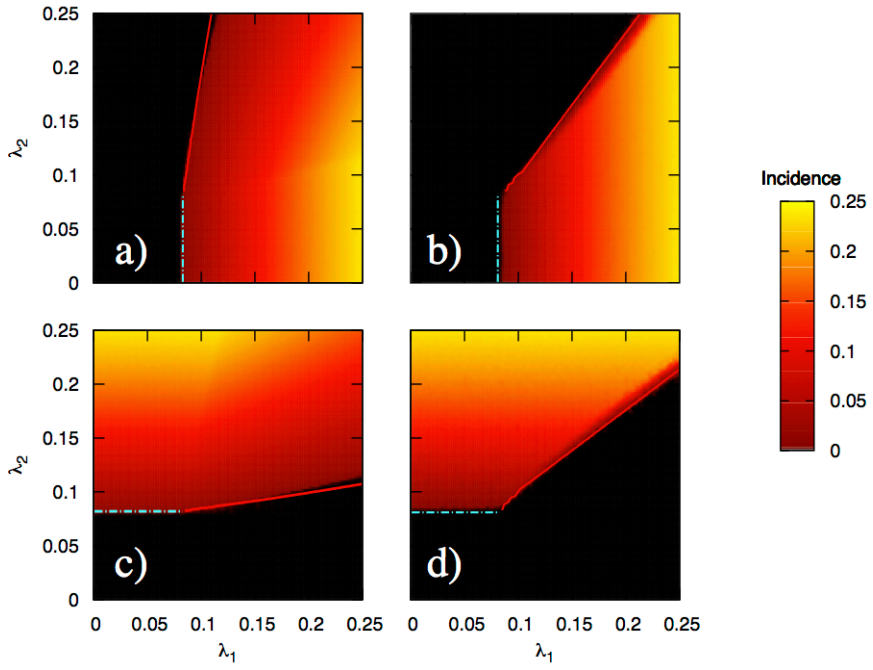

FIG. 6: (color online) Effect of degree correlations between the two scale-free networks on the steady prevalence levels. Dynamical parameters: $\mu_1 = \mu_2 = 0.75$, $\beta_1^a = \beta_2^a = 0$. The rest of parameters are irrelevant, as no ρ individual will appear in the system. Panels a and c: final prevalence of diseases 1 and 2, respectively for uncorrelated scale-free networks: $P(k,l) = P(k)P(l) = \alpha k^{-\gamma} l^{-\gamma}$. Panels b and d: final prevalence of diseases 1 and 2, respectively for fully correlated scale-free networks: $P(k,l) = \alpha\delta(k-l)k^{-\gamma}$. In both cases $\gamma = 2.5$.

framework, we propose a basic extension of an SIS model where the parameters defining the infectious and recovery transitions of one disease depend on the state of each node with respect to the conjugate disease, establishing in this way a coupling between both diffusion processes. Our modeling approach present different advantages with respect to previous models [36–39], as it simultaneously allows analytical derivations of the epidemic thresholds and a suitable description of the temporal evolution of the system. In addition, the model is easily "portable" from a classical model like SIS to any other, which is not a feature of all previous approaches [39]. Relevant enough for real cases, a SIS model is suitable to describe endemic diseases, and thus the influence on the prevalence level of each disease on the other can be tackled.

To illustrate the usefulness of our approach, let us discussion a real and relevant scenario in which two diseases coexist in the same host population: that of the interaction between AIDS and certain infections that spread from person to person and that are caused by opportunist pathogens usually associated to the immunodeficiency syndrome in advanced phases of the disease. Examples of these kind of diseases are respiratory disorders caused either by bacteria (like tubercle disease (TB), due to *Mycobacterium tuberculosis* [46] or fungi (like pneumonia caused by *Pneumocystis* [41]). Other examples of pathologies that appear commonly associated to advanced stages of AIDS are infections generated by the two variants of human herpes virus [40] and candidiasis [41], which is due to the fungal pathogen *Candida albicans*. The last two diseases affect typically the mouth area or the genitals, and depending of the area that they affect they can be transmitted after close contact (i.e. hands contact or saliva droplets interchange) or after sexual intercourses.

In some regions, the increase of the epidemiological risk related to some of the previous diseases after the irruption of HIV in the last decade of the XXth century has reached the dimension of a major threat for public health. The paradigmatic case is the recent boost of tuberculosis burden in sub-Saharian Africa, which is tightly related to the dramatic prevalence levels of HIV in that region, as it can be seen in figure 7. Given that our main purpose is to model these variations in the endemic prevalence level of one disease due to the irruption of another infection, our SIS-based modeling framework is the simplest way to recover an endemic equilibrium of a disease. In our case, this endemic equilibrium can be altered as a consequence of the irruption of the conjugate infection, in the same way that the appearance of HIV supposed an increase of tuberculosis burden in certain countries like the Republic of South Africa.

Figure 8 shows a comparison of the results obtained with our model with real data for the case of the Republic of South Africa during the period 1990-2011. In particular, we represent the results of a run of the mean field model with a set of parameters obtained through a Levemberg-Marquard [52] least-squares fitting approach (see Figure caption). The values of the parameters obtained through the fitting indicate that, on the one hand, that the driving effect in the interaction between both epidemics, in terms of our model, is the increasing susceptibility of individuals to get infected with one disease once infected with the other,

	TB prevalence $x10^5$ (1990 - 2000)	HIV prevalence (%) (1990 - 2000)	New HIV+, TB cases(%) (1990 - 2000)
Zambia	590 - 528	13.8 - 14.4	67 - 69
Malawi	354 - 357	7.8 - 13.8	51 - 69
Zimbabwe	242 - 328	13.6 - 26.2	69 - 92
South Africa	439 - 534	0.5 - 14.8	3.6 - 55

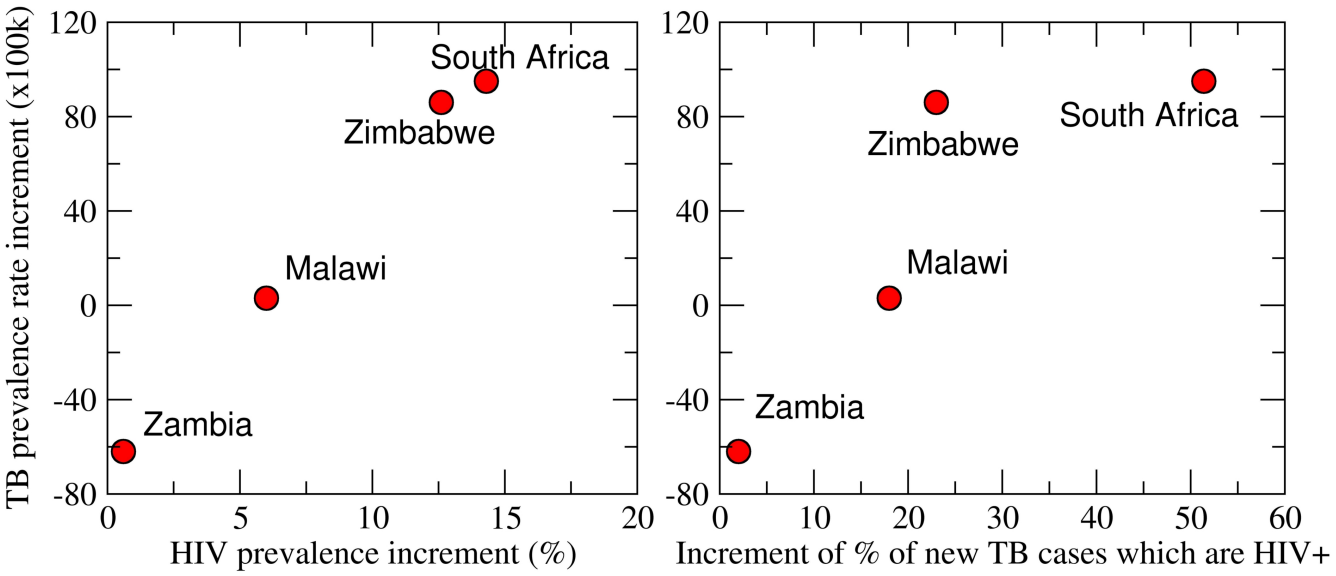

FIG. 7: (color online) Evolution of TB and HIV prevalences in most-populated, high HIV-burden countries in South Africa (population greater than 10 million inhabitant, HIV-prevalence in 2000 greater than 10%). The increase of HIV levels on the population in the last decade of the XXth century has been identified as the main cause of the increase of tuberculosis incidence and prevalence rates [42], as is evidenced not only by the correlation between HIV and TB prevalences but also by the correlation between TB burden and HIV-TB association frequencies.

rather than a significant increment in the spreading capabilities of double-infected individuals ($\beta_1^a > \beta_1^b$ and $\beta_2^a > \beta_2^b$). In addition, the values of $\eta_1 = 1.553$ and $\eta_2 = 2.729$ represent lower infectious periods for double-infected individuals, which is coherent with the increase of the mortality rates associated to TB-HIV co-infection [53]. This crucial factor in the interaction between both diseases, although it is not explicitly described by our model, also contributes to reduce the infectious periods of both diseases for TB-HIV co-infected individuals.

It is worth remarking that the actual interaction between both diseases is much more complex than the description provided by our model, as it involves many different phases of the natural history of the diseases, which are in turn much more complex than a simple SIS. Therefore, this makes the precise values of model parameters rather contingent. However, as the fit shows, our model remarkably captures the effects of one disease on the dynamics of the other. Therefore, this framework helps understanding what ingredients are basic and what others can be thrown out in a first approximation – it seems that for the real case here discussed, adding the coupling of the two diseases to simple models is effective enough to understand the coupled temporal evolution of both diseases. The previous comparison also indicates that modeling approaches like the one here introduced can be used to develop applied, data-driven models aimed at evaluating the increase in epidemiological risk due to AIDS high-prevalence levels on other diseases, like tuberculosis [50].

Summarizing, we have found that the epidemic thresholds of both diseases depend on both the underlying networks of contacts and on the dynamical parameters of each disease, similarly to what the classical scenario of single, uncoupled systems [17, 19, 28], in which the threshold vanishes for scale-free networks with $\gamma \leq 3$. This general result, however, has a remarkable exception unique to our scenario: either one of the pathogens impairs the spreading of the second one by making susceptible individuals immune to the second disease or the structure of the coupled system makes it possible to block the contagion processes when both diseases propagates over highly correlated scale-free networks. The conditions needed for the latter result to hold, also

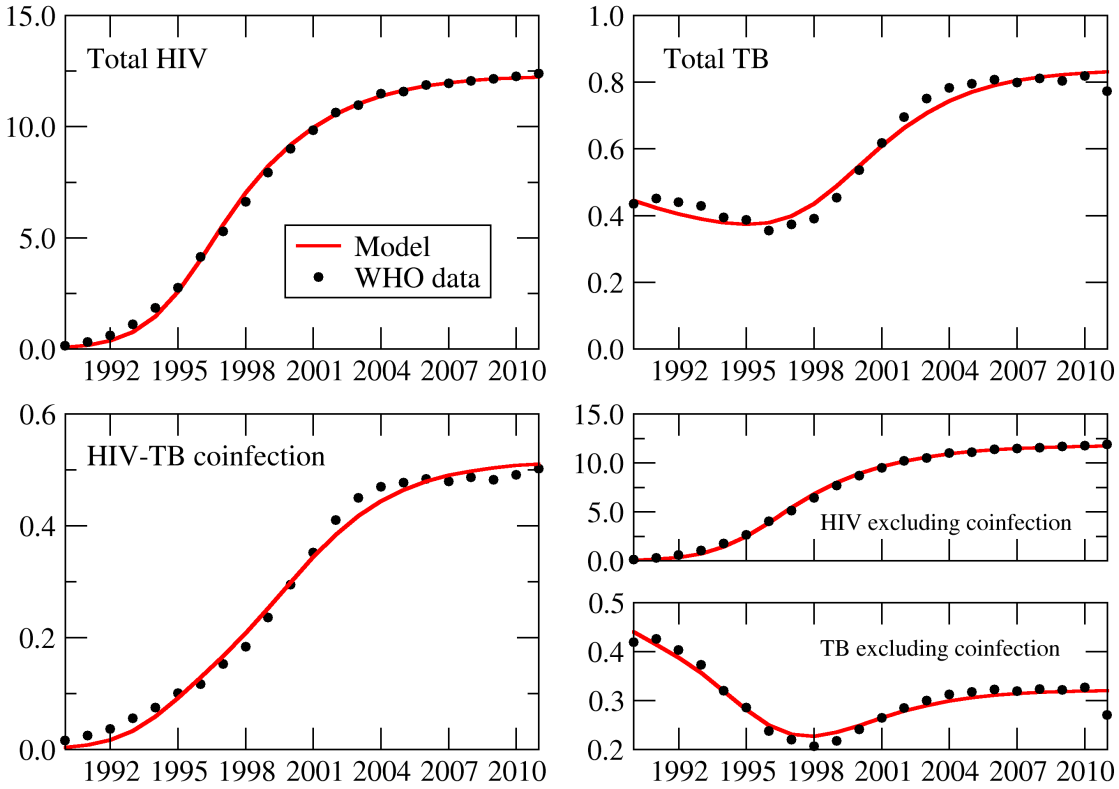

FIG. 8: (color online) Prevalence percentages for HIV and Tuberculosis in the Republic of South Africa from 1990 to 2011. In black, we represent the prevalence levels of both diseases, as available online at public databases for Tuberculosis [48] and HIV surveillance [49]. Even if the natural history of both pathologies are much more complex than a naive SIS model [50, 51], our model is able to reproduce the interactions between both diseases, and more specifically, the increment in TB's prevalence as a consequence of the irruption of HIV, mostly associated to co-infection. In the figure, in red, we represent the results of a run of the mean field model with the following parameters, obtained through a Levemberg-Marquard [52] least-squares fitting approach: $\langle k\rangle\lambda_1 = 6.166$, $\langle l\rangle\lambda_2 = 1.139$, $\beta_1^a = 21.40$, $\beta_2^a = 30.72$, $\beta_1^b = 0.03576$, $\beta_2^b = 1.807$, $\mu_1 = 30.75$, $\mu_2 = 5.361$, $\eta_1 = 1.553$, $\eta_2 = 2.729$. The first disease represents TB and the second one, HIV. The initial conditions are settled in 1988 for TB, (0.5% of prevalence of IS individuals) and, a year after, a 0.03% of SI individuals (HIV first carriers) is introduced. See the text for further discussions.

claimed in [37] though using another point of view, are not as unusual as one might think − for instance, it applies to the case in which two closely related pathogens (e.g., two strains of the same virus [33]) spread over the same population, sharing the same transmission paths (i.e. spreading over very correlated networks of contacts) and each one conferring to the host some level of immunity related to the conjugate infection. Finally, we note that as a consequence of the competition between the two diseases −or strains− for the same host population, although primary thresholds behave like in classical models and vanish at the thermodynamical limit, once one of the competing diseases becomes endemic (for example, disease 2, which yields $\sigma_2 > 0$), the threshold for an outbreak of the conjugate disease to occur (i.e., $\lambda_1^c(\sigma_2 > 0)$) is not null anymore even in the thermodynamic limit. This worthily implies that the region of coexistence of both diseases can never be the whole parameter space, also in agreement with other previous results pointing in the same direction [37], even when the two diseases spread through infinite scale-free networks.

TABLE III: Linear stability analysis of fixed point $(\rho_1, \rho_2, \rho) = (0, 0, 0)$

Eigen-value	Eigen-vector (ρ_1, ρ_2, ρ)	Stability condition (epidemic threshold)
$\xi_1 = \lambda_1 k_o - \mu_1$	$\vec{\psi_1} = (1, 0, 0)$	$\lambda_1 < \lambda_{1_i}^c = \mu_1/k_o$
$\xi_2 = \lambda_2 l_o - \mu_2$	$\vec{\psi_2} = (0, 1, 0)$	$\lambda_2 < \lambda_{2_i}^c = \mu_2/l_o$
$\xi_3 = -(\eta_1\mu_1 + \eta_2\mu_2)$	$\vec{\psi_3} = \left(-\frac{\eta_2\mu_2+\beta_1^b\lambda_1 k_o}{(\lambda_1 k_o-\mu_1)+(\eta_1\mu_1+\eta_2\mu_2)}, -\frac{\eta_1\mu_1+\beta_2^b\lambda_2 l_o}{(\lambda_2 l_o-\mu_2)+(\eta_1\mu_1+\eta_2\mu_2)}, 1\right)$	always stable

Appendix A: Epidemic thresholds on regular networks

In the particular case in which both networks are homogeneous graphs, an independent derivation of the epidemic threshold can be obtained by a linear stability analysis. In that case, for which $P(k, l) = \delta(k - k_o)\delta(l - l_o)$, the dynamics can be described by the following system of four equations:

$$\begin{aligned}
\dot{s} &= -k_o\lambda_1 s\rho_1 - l_o\lambda_2 s\rho_2 - k_o\beta_1^b\lambda_1 s\rho - l_o\beta_2^b\lambda_2 s\rho + \mu_1\rho_1 + \mu_2\rho_2,\\
\dot{\rho_1} &= k_o\lambda_1 s\rho_1 + k_o\beta_1^b\lambda_1 s\rho - l_o\beta_2^a\lambda_2\rho_2\rho_1 - l_o\beta_2^a\beta_2^b\lambda_2\rho_1\rho - \mu_1\rho_1 + \eta_2\mu_2\rho,\\
\dot{\rho_2} &= l_o\lambda_2 s\rho_2 + l_o\beta_2^b\lambda_2 s\rho - k_o\beta_1^a\lambda_1\rho_1\rho_2 - k_o\beta_1^a\beta_1^b\lambda_1\rho_2\rho - \mu_2\rho_2 + \eta_1\mu_1\rho,\\
\dot{\rho} &= k_o\beta_1^a\lambda_1\rho_1\rho_2 + l_o\beta_2^a\lambda_2\rho_1\rho_2 + k_o\beta_1^a\beta_1^b\lambda_1\rho_2\rho + l_o\beta_2^a\beta_2^b\lambda_2\rho_1\rho - (\eta_1\mu_1 + \eta_2\mu_2)\rho,
\end{aligned}$$

one of which is linearly dependent of the rest. Thus, we will only analyze the system constituted by the three last equations and use $s = 1 - \rho_1 - \rho_2 - \rho$. In order to perform a linear stability analysis we first linearize the system around the equilibrium point and we calculate the Jacobian to get:

$$J = \begin{vmatrix} \lambda_1 k_o - \mu_1 & 0 & k_o\beta_1^b\lambda_1 + \eta_2\mu_2 \\ 0 & \lambda_2 l_o - \mu_2 & l_o\beta_2^b\lambda_2 + \eta_1\mu_1 \\ 0 & 0 & -(\eta_1\mu_1 + \eta_2\mu_2) \end{vmatrix} \tag{A1}$$

which, taking advantage of the fact that the Jacobian itself is just the product of the elements in the diagonal, yields the stability conditions detailed in table III.

If we look carefully at the results sketched in table III, we firstly recognize the appearance of a couple of critical values for the infectiousnesses $\lambda_{1_i}^c$ and $\lambda_{2_i}^c$ which will be referred to in what follows as the primary thresholds of their respective diseases, just like in the general case described in the main text. These threshold values stand for the *minimum values of the infectiousnesses that yield epidemic outbreaks after the introduction of infinitesimal seeds of infected individuals of each disease in an initially healthy population*. Therefore, the condition $\lambda_1 > \lambda_{1_i}^c$ must be verified in order to have an epidemic outbreak for the first disease once an infinitesimal seed $(\rho_1, \rho_2, \rho) = (\epsilon, 0, 0)$ has been introduced on a system being at the disease-free fixed point $(\rho_1, \rho_2, \rho) = (0, 0, 0)$. On the other hand, the condition $\lambda_{2_i}^c$ plays an equivalent role for the second disease with respect to a seed $(\rho_1, \rho_2, \rho) = (0, \epsilon, 0)$.

The fixed point $(\rho_1, \rho_2, \rho) = (0, 0, 0)$ is, strictly speaking, not the only possible disease-free fixed point in our model. Other two partially disease-free fixed points can exist: a first fixed point in which disease 1 is installed in the system at a certain prevalence π_1 whilst disease 2 is absent $(\rho_1, \rho_2, \rho) = (\pi_1, 0, 0)$ and its cognate $(\rho_1, \rho_2, \rho) = (0, \pi_2, 0)$, for which there is no individual infected with disease 1. As we are going to show, the stability of these fixed points depends on the prevalence fractions π_1 and π_2, which are the stationary proportions of sick individuals of each disease:

$$\pi_1 = \frac{\lambda_1 k_o - \mu_1}{\lambda_1 k_o} \tag{A2}$$

$$\pi_2 = \frac{\lambda_2 l_o - \mu_2}{\lambda_2 l_o} \tag{A3}$$

Considering that, let us study the stability of the first fixed point $(\rho_1, \rho_2, \rho) = (\pi_1 = \frac{\lambda_1 k_o - \mu_1}{\lambda_1 k_o}, 0, 0)$ as a function of λ_1: the Jacobian, around this fixed point takes the following form:

$$J = \begin{vmatrix} (\mu_1 - \lambda_1 k_o) & (\mu_1 - \lambda_1 k_o)(1 + \beta_2^a \frac{\lambda_2 l_o}{\lambda_1 k_o}) & \beta_1^b \lambda_1 k_o + \eta_2 \mu_2 + (\mu_1 - \lambda_1 k_o)(\beta_1^b + 1 + \beta_2^a \beta_2^b \frac{\lambda_2 l_o}{\lambda_1 k_o}) \\ 0 & (\lambda_2 l_o - \mu_2) + (\mu_1 - \lambda_1 k_o)(\frac{\lambda_2 l_o}{\lambda_1 k_o} + \beta_1^a) & \beta_2^b \mu_1 \frac{\lambda_2 l_o}{\lambda_1 k_o} + \eta_1 \mu_1 \\ 0 & (\lambda_1 k_o - \mu_1)(\beta_2^a \frac{\lambda_2 l_o}{\lambda_1 k_o} + \beta_1^a) & (\lambda_1 k_o - \mu_1)\beta_2^a \beta_2^b \frac{\lambda_2 l_o}{\lambda_1 k_o} - (\eta_1 \mu_1 + \eta_2 \mu_2) \end{vmatrix} \quad \text{(A4)}$$

By solving the equation derived from imposing that $J = 0$, we obtain the values of the parameters leading to stability inversion. As it can be shown at naked eye, $(\mu_1 - \lambda_1 k_o)$ is the eigenvalue ξ_1 associated to the eigenvector $\vec{\psi_1} = (1, 0, 0)$, and the condition $\xi_1 = 0$ yields again the same condition $\lambda_1 = \mu_1 / k_o$, thus defining the threshold of the classical SIS model. Regarding the other two eigenvalues ξ_2 and ξ_3, the result is more cumbersome. Despite of that, the vanishing of the 2x2 determinant of the right-inferior corner of the Jacobian matrix A4 yields:

$$\lambda_2 = \lambda_{2ii}^c = \frac{\lambda_1 k_o}{l_o} \frac{\eta_2 \mu_2 ((\beta_1^a (\lambda_1 k_o - \mu_1) + \mu_2) + \eta_1 \mu_1 \mu_2}{\mu_1 (\eta_1 \mu_1 + \eta_2 \mu_2) + (\lambda_1 k_o - \mu_1)(\beta_1^a \beta_2^a \beta_2^b (\lambda_1 k_o - \mu_1) + \beta_2^a \beta_2^b \mu_2 + \eta_1 \mu_1 \beta_2^a + \beta_1^a \beta_2^b \mu_1)}, \quad \text{(A5)}$$

to which the general expression presented in the main text for the epidemic threshold reduces when $P(k, l) = \delta(k - k_o)\delta(l - l_o)$. The agreement between numerical simulations and the analytic expression of the threshold presented here is only accurate when $\lambda_1 k_o \simeq \mu_1$, and the reason is easily understandable. Let us compare the reaction of the system to the introduction of a small seed of ρ_2 individuals when both diseases are absent ($(\rho_1, \rho_2, \rho) = (0, 0, 0)$, case 1) or when the first disease was already installed in the system ($(\rho_1, \rho_2, \rho) = (\pi_1, 0, 0)$, case 2). As we have argued in the precedent sections, the epidemic threshold is different in each case, and the reason is simply the presence, in the second case, of a fraction π_1 of ρ_1 of individuals for which the infectiousness and recovery rates for disease 2 are different with respect to the rest of individuals. As a consequence, the mean values of the dynamical parameters averaged over the whole population $\langle \lambda_2 \rangle$ and $\langle \mu_2 \rangle$, are different in both cases and will yield different values for the epidemic threshold. Thus, in order to accurately evaluate the secondary threshold for disease 2 it is essential to know with enough precision the prevalence π_1 corresponding to a single SIS model, as a function of λ_1. The problem arises from the fact that, precisely, the derivation of A5 explicitly assumes that the bijection between π_1 and λ_1 is governed by the mean field stationary expression A2 which is only precise when $\lambda_1 k_o \simeq \mu_1$ [25]. In fact, a way to rebuild a more accurate secondary threshold curve can be achieved if, from equation A2 we substitute λ_1 as a function of π_1, and then introduce the so obtained expression into A5 to get:

$$\lambda_{2ii}^c(\pi_1) = \frac{1}{l_o} \frac{\eta_2 \mu_2 (\beta_1^a \frac{\mu_1 \pi_1}{(1-\pi_1)} + \mu_2) + \eta_1 \mu_1 \mu_2}{(1 - \pi_1)(\eta_1 \mu_1 + \eta_2 \mu_2) + \pi_1 (\beta_1^a \beta_2^a \beta_2^b \frac{\mu_1 \pi_1}{(1-\pi_1)} + \beta_2^a \beta_2^b \mu_2 + \eta_1 \mu_1 \beta_2^a + \beta_1^a \beta_2^b \mu_1)} \quad \text{(A6)}$$

which allows to evaluate directly the threshold as a function of π_1 rather than of λ_1. Thus, by introducing in equation A6 the π_1 values obtained from the simulations instead of the theoretical prediction of the mean field (equation A2), we recover the curves for the secondary threshold represented with red lines in Figures 2 and 3 of the main text, in quantitative agreement with results from simulations.

Obviously, the same arguments stand for the secondary threshold of the first disease, which obeys the following expression:

$$\lambda_{1ii}^c(\pi_2) = \frac{1}{k_o} \frac{\eta_1 \mu_1 (\beta_2^a \frac{\mu_2 \pi_2}{(1-\pi_2)} + \mu_1) + \eta_2 \mu_2 \mu_1}{(1 - \pi_2)(\eta_2 \mu_2 + \eta_1 \mu_1) + \pi_2 (\beta_2^a \beta_1^a \beta_1^b \frac{\mu_2 \pi_2}{(1-\pi_2)} + \beta_1^a \beta_1^b \mu_1 + \eta_2 \mu_2 \beta_1^a + \beta_2^a \beta_1^b \mu_2)} \quad \text{(A7)}$$

When the networks are heterogeneous, this reformulation of the threshold curves as a function of π_1 or π_2 can not be done straightforwardly as no analytical bijection $\lambda_1(\pi_1)$ or $\lambda_2(\pi_2)$ can be reached. The best we can do is to use a numerically built-up relationship $\lambda_1(\theta_1)$ (or $\lambda_2(\theta_2)$), and introduce it into the general expression for the threshold. Although the accuracy of the curves for the secondary threshold is very satisfactory in Fig. 4, we identify this effect to be the source of the slight divergence between the analytical and numerical secondary thresholds shown in Fig. 6.

Appendix B: Vanishing conditions for epidemic thresholds

Here we provide a systematic analysis of the behavior of the secondary threshold in our model for large scale-free networks. In particular, we inspect whether the coupling between the spreading of the two diseases in the terms described in our model can modify the classical, single-disease scheme, and, if so, under what conditions. The epidemic threshold for the first disease in our model reads as:

$$\lambda_1^c(\sigma_2) = \mu_1 \frac{\langle k \rangle}{\sum_{k,l} P(k,l) \frac{k^2 l^2 \sigma_2^2 \beta_2^a \beta_1^a \beta_1^b + l k^2 \sigma_2 (\eta_2 \mu_2 \beta_1^a + \beta_1^b (\beta_1^a \mu_1 + \beta_2^a \mu_2)) + k^2 \mu_2 (\eta_1 \mu_1 + \eta_2 \mu_2)}{l^2 \sigma_2^2 \beta_2^a \eta_1 + l \sigma_2 (\eta_1 \mu_1 + \eta_2 \mu_2 + \beta_2^a \eta_1 \mu_2) + \mu_2 (\eta_1 \mu_1 + \eta_2 \mu_2)}} \tag{B1}$$

and we have to address its behavior in the limit $N \to \infty$. Substituting sums by integrals in Eq. (B1), one gets:

$$\lim_{N\to\infty} \lambda_1^c(\sigma_2) = \lim_{(k_{max}, l_{max})\to\infty} \mu_1 \frac{\int_{k_{min}}^{k_{max}} \int_{l_{min}}^{l_{max}} P(k,l) k \, dk \, dl}{\int_{k_{min}}^{k_{max}} \int_{l_{min}}^{l_{max}} P(k,l) \frac{k^2 l^2 \sigma_2^2 \beta_2^a \beta_1^a \beta_1^b + l k^2 \sigma_2 (\eta_2 \mu_2 \beta_1^a + \beta_1^b (\beta_1^a \mu_1 + \beta_2^a \mu_2)) + k^2 \mu_2 (\eta_1 \mu_1 + \eta_2 \mu_2)}{l^2 \sigma_2^2 \beta_2^a \eta_1 + l \sigma_2 (\eta_1 \mu_1 + \eta_2 \mu_2 + \beta_2^a \eta_1 \mu_2) + \mu_2 (\eta_1 \mu_1 + \eta_2 \mu_2)} dk \, dl}. \tag{B2}$$

To study the behavior of the threshold in the thermodynamic limit, we present here an analysis which is essentially based on the following result, which proof is an exercise of elementary algebra that we present for the sake of completeness in the last appendix. Given two polynomials $P(k)$, $Q(k)$, we have that:

$$\left| \lim_{k_{max}\to\infty} \int_{k_{min}}^{k_{max}} \frac{P(k)}{Q(k)} dk \right| = \infty \leftrightarrow deg(Q) - deg(P) \leq 1 \tag{B3}$$

Focusing on scale-free connectivity distributions, we will distinguish two different scenarios in this section: uncorrelated and totally correlated layers. In the first case, both networks present a scale free distribution in which the connectivity of a node in a layer is essentially independent of its degree on the other layer, in such a way that the composed connectivity distribution verifies $P(k,l) = C_o k^{-\gamma} l^{-\Gamma}$. Instead, in the second case, although both layers are also scale free networks, the degree of any given node in both layers is forced to be the same. Therefore, nodes which are hubs in a layer are so in the other, and the composed degree distribution is $P(k,l) = C_o \delta(k-l) k^{-\gamma}$. In addition, we assume that both γ and Γ exponents are rational, hence, we can write $\gamma = w/x$ and $\Gamma = y/z$ with $(w,x,y,z) \in \mathbb{N}$. By addressing these two opposite scenarios, our aim is to characterize the difference, in terms of the spreading dynamics, between the coupling of two diseases that spread by independent means –which will give place to different networks of contacts– and the coupling of two related diseases –or variations of the same disease– that spread following the very same mechanisms and, thus, they do so over highly correlated networks of contacts.

1. Uncorrelated scale free layers

If we substitute $P(k,l) = C_o k^{-\gamma} l^{-\Gamma}$ into eq. B2, we can factorize the double integrals into independent terms:

$$\lim_{N\to\infty} \lambda_1^c(\sigma_2) = \lim_{(k_{max}, l_{max})\to\infty} \mu_1 \frac{\int_{k_{min}}^{k_{max}} k^{1-\gamma} dk \int_{l_{min}}^{l_{max}} l^{-\Gamma} dl}{\int_{k_{min}}^{k_{max}} k^{2-\gamma} dk \int_{l_{min}}^{l_{max}} \frac{l^2 \sigma_2^2 \beta_2^a \beta_1^a \beta_1^b + l \sigma_2 (\eta_2 \mu_2 \beta_1^a + \beta_1^b (\beta_1^a \mu_1 + \beta_2^a \mu_2)) + \mu_2 (\eta_1 \mu_1 + \eta_2 \mu_2)}{l^\Gamma \left(l^2 \sigma_2^2 \beta_2^a \eta_1 + l \sigma_2 (\eta_1 \mu_1 + \eta_2 \mu_2 + \beta_2^a \eta_1 \mu_2) + \mu_2 (\eta_1 \mu_1 + \eta_2 \mu_2) \right)} dl} \tag{B4}$$

The condition for the numerator to diverge is $\gamma \leq 2 \vee \Gamma \leq 1$. These conditions are verified by networks whose mean connectivity diverges in the thermodynamic limit. For this reason, networks with those small exponents neither are reasonable systems to be used to describe any information diffusion process over them nor are found in real systems. Taking this into account, we will restrict our analysis to the more epidemiologically relevant scenario in which $\gamma > 2$ and $\Gamma > 2$, although our reasoning is trivially generalizable to any value of the exponents.

Thus, in the scenario $\gamma > 2$ and $\Gamma > 2$, the numerator remains always finite and the only phenomenon of interest that could be found is an eventual vanishing of the threshold due to a divergence in the denominator –$D(k,l)$ in what follows–. $D(k,l)$ can be factorized to give $D(k,l) = D_1(k) D_2(l)$, as it can be seen from Eq. B4. The integral in k, $D_1(k)$ will diverge if and only if $\gamma \leq 3$, but the integral in l, $D_2(l)$, might independently diverge under some conditions. That situation would suppose the vanishing of the threshold of the first disease as a consequence of its coupling to the second rather than to internal, dynamical or topological features. To find out the conditions for $D_2(l)$, lets make the following change of variable:

$$m = l^{1/z} \tag{B5}$$

so as to change the dependence of the denominator $D(k,l) = D_1(k) D_2(l)$ in Eq. B4 to $D(k,m) = D_1(k) D_2(m)$:

$$\lim_{N\to\infty} \lambda_1^c(\sigma_2) = \lim_{(k_{max}, l_{max})\to\infty} \mu_1 \frac{\int_{k_{min}}^{k_{max}} k^{1-\gamma} dk}{\int_{k_{min}}^{k_{max}} k^{2-\gamma} dk \int_{l_{min}^{1/z}}^{l_{max}^{1/z}} \frac{\left(m^{2z} \sigma_2^2 \beta_2^a \beta_1^a \beta_1^b + m^z \sigma_2 (\eta_2 \mu_2 \beta_1^a + \beta_1^b (\beta_1^a \mu_1 + \beta_2^a \mu_2)) + \mu_2 (\eta_1 \mu_1 + \eta_2 \mu_2) \right) z m^{z-1}}{m^y \left(m^{2z} \sigma_2^2 \beta_2^a \eta_1 + m^z \sigma_2 (\eta_1 \mu_1 + \eta_2 \mu_2 + \beta_2^a \eta_1 \mu_2) + \mu_2 (\eta_1 \mu_1 + \eta_2 \mu_2) \right)} dm} \tag{B6}$$

TABLE IV: Divergence conditions for $D_2(m)$ for disease 1. Case 1: uncorrelated scale free layers $P(k,l) = C_o k^{-\gamma} l^{-\Gamma}$, $\gamma = (w/x)$, $\Gamma = (y/z)$.

$(\beta_1^a, \beta_1^b, \beta_2^a)$ parameters	$deg(Q) - deg(P)$ in $D_2(m) = P(m)/Q(m)$	Divergence condition
$(\beta_1^a, \beta_1^b, \beta_2^a)$ $(\beta_1^a, \beta_1^b, 0)$ $(\beta_1^a, 0, 0)$	$y - z + 1$	$\gamma \leq 3 \vee \Gamma \leq 1$
$(0, \beta_1^b, \beta_2^a)$ $(\beta_1^a, 0, \beta_2^a)$ $(0, \beta_1^b, 0)$ $(0, 0, 0)$	$y + 1$	$\gamma \leq 3 \vee \Gamma \leq 0$
$(0, 0, \beta_2^a)$	$y + z + 1$	$\gamma \leq 3 \vee \Gamma \leq -1$

The last expression has the advantage that the argument of the integral in m, $D_2(m)$ is just the quotient of two polynomials, and thus, its behavior in the limit $l_{max} \to \infty$ is governed by Eq. (B3) and depends only on the difference of degrees of the denominator and the numerator. If

$$D_2(m) = \int_{l_{min}^{1/z}}^{l_{max}^{1/z}} \frac{\left(m^{2z}\sigma_2^2\beta_2^a\beta_1^a\beta_1^b + m^z\sigma_2(\eta_2\mu_2\beta_1^a + \beta_1^b(\beta_1^a\mu_1 + \beta_2^a\mu_2)) + \mu_2(\eta_1\mu_1 + \eta_2\mu_2)\right) z m^{z-1}}{m^y\left(m^{2z}\sigma_2^2\beta_2^a\eta_1 + m^z\sigma_2(\eta_1\mu_1 + \eta_2\mu_2 + \beta_2^a\eta_1\mu_2) + \mu_2(\eta_1\mu_1 + \eta_2\mu_2)\right)} dm = \int_{l_{min}^{1/z}}^{l_{max}^{1/z}} \frac{P(m)}{Q(m)} dm \tag{B7}$$

we have that –in the general case in which none of the β and η parameters vanishes– $deg(Q) - deg(P) = 1 + y - z$, and hence, the conditions for $D_2(m)$ to diverge are

$$\lim_{(k_{max}, l_{max}) \to \infty} \int_{l_{min}^{1/z}}^{l_{max}^{1/z}} \frac{P(m)}{Q(m)} dm = \infty \leftrightarrow y - z + 1 \leq 1 \leftrightarrow \Gamma = y/z \leq 1 \tag{B8}$$

Therefore, in the region of interest $\gamma > 2 \wedge \Gamma > 2$, the factor $D_2(m)$ can not diverge and make the threshold to vanish. It is worth noticing that the condition $\Gamma < 1$ does not guarantee the vanishing of the threshold, as it makes also the numerator to diverge. Expression B8 is valid for the case in which none of the β and η parameters of the model vanishes. If this is not the case, i.e., if some of the infectiousness variations β do vanish −the rest of the parameters can not do that within a realistic epidemiological framework−, the degrees of the numerator and the denominator in Eq. B7 could vary. In table IV we address systematically all the possible combinations of null parameters, and the composed conditions yielding a vanishing threshold for each case.

Once again, we see that, whatever the interacting scheme between both diseases is, the denominator remains always finite provided that $\Gamma > 2$. In conclusion, if no degree correlation is introduced between layers, and for realistic systems characterized by double power laws verifying $\gamma > 2 \wedge \Gamma > 2$, the behavior of the thresholds in the thermodynamic limit is essentially the same of the uncoupled systems: the threshold associated to the first disease vanishes if and only if the exponent of its own network verifies $\gamma \leq 3$, whatever the exponent of the second network. The coupling will introduce, in general, only a finite pre-factor. The symmetric situation obviously stands for the threshold of the second disease.

2. Totally correlated scale free layers

If we consider the case in which $P(k,l) = C_o \delta(k-l) k^{-\gamma}$, where $\gamma = w/x$ with $(w,x) \in \mathbb{N}$, the epidemic threshold reads as:

$$\lim_{N \to \infty} \lambda_1^c(\sigma_2) = \lim_{(k_{max}, l_{max}) \to \infty} \mu_1 \frac{\int_{k_{min}}^{k_{max}} k^{1-\gamma} dk}{\int_{k_{min}}^{k_{max}} \frac{k^2\sigma_2^2\beta_2^a\beta_1^a\beta_1^b + k\sigma_2(\eta_2\mu_2\beta_1^a + \beta_1^b(\beta_1^a\mu_1 + \beta_2^a\mu_2)) + \mu_2(\eta_1\mu_1 + \eta_2\mu_2)}{k^{\gamma-2}\left(k^2\sigma_2^2\beta_2^a\eta_1 + k\sigma_2(\eta_1\mu_1 + \eta_2\mu_2 + \beta_2^a\eta_1\mu_2) + \mu_2(\eta_1\mu_1 + \eta_2\mu_2)\right)} dk} \tag{B9}$$

hence, we do not recover the factorization of the denominator previously observed. Instead, after changing the variable to $m = k^{1/x}$, we get the following expression:

$$\lim_{N \to \infty} \lambda_1^c(\sigma_2) = \lim_{(k_{max}) \to \infty} \mu_1 \frac{\int_{k_{min}}^{k_{max}} k^{1-\gamma} dk}{\int_{k_{min}^{1/x}}^{k_{max}^{1/x}} \frac{\left(m^{2x}\sigma_2^2\beta_2^a\beta_1^a\beta_1^b + m^x\sigma_2(\eta_2\mu_2\beta_1^a + \beta_1^b(\beta_1^a\mu_1 + \beta_2^a\mu_2)) + \mu_2(\eta_1\mu_1 + \eta_2\mu_2)\right) x m^{x-1}}{m^{w-2x}\left(m^{2x}\sigma_2^2\beta_2^a\eta_1 + m^x\sigma_2(\eta_1\mu_1 + \eta_2\mu_2 + \beta_2^a\eta_1\mu_2) + \mu_2(\eta_1\mu_1 + \eta_2\mu_2)\right)} dm} \tag{B10}$$

TABLE V: Divergence conditions for $D_2(m)$ for disease 1. Case 2: totally correlated scale free layers $P(k,l) = C_o\delta(k-l)k^{-\gamma}, \gamma = (w/x)$.

$(\beta_1^a, \beta_1^b, \beta_2^a)$ parameters	$deg(Q) - deg(P)$ in $D_2(m) = P(m)/Q(m)$	Divergence condition
$(\beta_1^a, \beta_1^b, \beta_2^a)$ $(\beta_1^a, \beta_1^b, 0)$ $(\beta_1^a, 0, 0)$	$w - 3x + 1$	$\gamma \leq 3$
$(0, \beta_1^b, \beta_2^a)$ $(\beta_1^a, 0, \beta_2^a)$ $(0, \beta_1^b, 0)$ $(0, 0, 0)$	$w - 2x + 1$	$\gamma \leq 2$
$(0, 0, \beta_2^a)$	$w - x + 1$	$\gamma \leq 1$

In this expression, the numerator diverges for $\gamma \leq 2$. In turn, the denominator:

$$D(m) = \int_{k_{min}^{1/x}}^{k_{max}^{1/x}} \frac{\left(m^{2x}\sigma_2^2\beta_2^a\beta_1^a\beta_1^b + m^x\sigma_2(\eta_2\mu_2\beta_1^a + \beta_1^b(\beta_1^a\mu_1 + \beta_2^a\mu_2)) + \mu_2(\eta_1\mu_1 + \eta_2\mu_2)\right) xm^{x-1}}{m^{w-2x}\left(m^{2x}\sigma_2^2\beta_2^a\eta_1 + m^x\sigma_2(\eta_1\mu_1 + \eta_2\mu_2 + \beta_2^a\eta_1\mu_2) + \mu_2(\eta_1\mu_1 + \eta_2\mu_2)\right)} dm = \int_{k_{min}^{1/x}}^{k_{max}^{1/x}} \frac{P(m)}{Q(m)} dm \tag{B11}$$

diverges, according to equation B3, if and only if $deg(Q) - deg(P) \leq 1$. In the general case in which none of the β parameters vanishes, we have that $deg(Q) - deg(P) = w - 3x + 1$, and thus:

$$\lim_{N\to\infty} \lambda_1^c(\sigma_2) = 0 \leftrightarrow \gamma \leq 3 \tag{B12}$$

As in the previous case, different combination of null β parameters can change this result, as it can be seen in Table V. Here, the phenomenology is remarkable different for all the cases in which at least one of the two variations of disease 1 infectiousness, β_1^a or β_1^b, cancel (except for the case $\beta_2^a = \beta_1^b = 0$ but $\beta_1^a \neq 0$, for which eq. B12 also stands). In those cases, $\theta > 0$ guarantees that, provided that $\gamma > 2$, no threshold vanishing is observed in the thermodynamic limit, even when the exponent is within the interval $2 < \gamma \leq 3$. In the case in which $\beta_1^a = \beta_1^b = \beta_2^a = 0$, the situation will be reciprocal, and thus, the epidemic threshold of the second disease will not vanish either for $\gamma > 2$.

Appendix C: Proof of eq. B3

Given two polynomials $P(k)$, $Q(k)$, we have to proof that

$$\left| \lim_{k_{max}\to\infty} \int_{k_{min}}^{k_{max}} \frac{P(k)}{Q(k)} dk \right| = \infty \leftrightarrow deg(Q) - deg(P) \leq 1 \tag{C1}$$

First, we have that, if $deg(P) \geq deg(Q)$ the integral diverges, as the argument of the integral can be expressed in that case as:

$$\frac{P(k)}{Q(k)} = C(k) + \frac{P'(k)}{Q'(k)} \tag{C2}$$

with $deg(P') < deg(Q')$ and $deg(C) \geq 0$. When substituting the last expression into eq.B3, the integral in $C(k)$ automatically diverges. Therefore, to prove this result for the case in which $deg(P) < deg(Q)$, let us consider the general decomposition of $Q(k)$:

$$Q(k) = Q_o \prod_{i=1}^{i^*} (k - a_i)^{n_i} \prod_{j=1}^{j^*} (k^2 + b_j k + c_j)^{m_j} \tag{C3}$$

where Q_o is a constant, $k_{min} > 0$ and $b_j^2 - 4c_j < 0 \; \forall j$. The values i^* and j^* stand for the number of different elemental factors of first and second order, respectively. So, the degree of the polynomial reads as follows:

$$deg(Q) = \sum_{i=1}^{i^*} n_i + 2\sum_{j=1}^{j^*} m_j, \tag{C4}$$

where n_i and m_j denote the multiplicity of each of the factors of first and second order, respectively. The factorization of $Q(k)$ yields the following decomposition of the quotient $P(k)/Q(k)$ into partial fractions:

$$\int_{k_{min}}^{k_{max}} \frac{P(k)}{Q(k)}dk = \sum_{i=1}^{i^*}\sum_{n=1}^{n_i}\int_{k_{min}}^{k_{max}} \frac{A_{i,n}}{(k+a_i)^n}dk + \sum_{j=1}^{j^*}\sum_{m=1}^{m_j}\int_{k_{min}}^{k_{max}} \frac{B_{j,m}k + C_{j,m}}{(k^2+b_jk+c_j)^m}dk \tag{C5}$$

where the coefficients $A_{i,n}, B_{j,m}, C_{j,m}$ have to be calculated by expanding this expression into a single fraction, and comparing the coefficients of the numerator obtained with those of $P'(k) = P(k)/Q_o$. With the aim of understanding what are the conditions that make these partial integrals to diverge, let us analyze them term by term. The first sum yields logarithmic and rational functions:

$$\sum_{i=1}^{i^*}\sum_{n=1}^{n_i}\int_{k_{min}}^{k_{max}} \frac{A_{i,n}}{(k+a_i)^n}dk = \sum_{i=1}^{i^*} A_{i,1}\ln\left(\frac{k_{max}+a_i}{k_{min}+a_i}\right) + \sum_{i=1|n_i>1}^{i^*}\sum_{n=2}^{n_i}\frac{-A_{i,n}}{(n-1)}\left(\frac{1}{(k_{min}+a_i)^{n-1}} - \frac{1}{(k_{max}+a_i)^{n-1}}\right) \tag{C6}$$

and, in the limit $k_{max}\to\infty$, only the logarithmic term diverges:

$$\lim_{k_{max}\to\infty}\sum_{i=1}^{i^*}\sum_{n=1}^{n_i}\int_{k_{min}}^{k_{max}} \frac{A_{i,n}}{(k+a_i)^n}dk = \sum_{i=1}^{i^*} A_{i,1}\ln(k_{max}) + \vartheta \tag{C7}$$

where ϑ stands for a finite term, negligible when compared to $\ln(k_{max})$. On the other hand, the second sum in eq. C5 can be rewritten as:

$$\sum_{j=1}^{j^*}\sum_{m=1}^{m_j}\int_{k_{min}}^{k_{max}} \frac{B_{j,m}k + C_{j,m}}{(k^2+b_jk+c_j)^m}dk = \sum_{j=1}^{j^*}\sum_{m=1}^{m_j}\frac{B_{j,m}}{2}\int_{k_{min}}^{k_{max}} \frac{2k+b_j}{(k^2+b_jk+c_j)^m}dk + \left(C_{j,m} - \frac{B_{j,m}}{2}\right)\int_{k_{min}}^{k_{max}}\frac{dk}{(k^2+b_jk+c_j)^m}dk \tag{C8}$$

In turn, the integrals in the first sum of eq. C8 can be easily solved:

$$\begin{array}{l}\sum_{j=1}^{j^*}\sum_{m=1}^{m_j}\frac{B_{j,m}}{2}\int_{k_{min}}^{k_{max}}\frac{2k+b_j}{(k^2+b_jk+c_j)^m}dk = \sum_{j=1}^{j^*}\frac{B_{j,m}}{2}\ln\frac{(k_{max}^2+b_jk_{max}+c_j)}{(k_{min}^2+b_jk_{min}+c_j)} + \\ + \sum_{j=1|m_j>1}^{j^*}\sum_{m=1}^{m_j}\frac{B_{j,m}}{2}\left(\frac{1}{k_{min}^2+b_jk_{min}+c_j} - \frac{1}{k_{max}^2+b_jk_{max}+c_j}\right)\end{array} \tag{C9}$$

and, again, when taking the limit $k_{max}\to\infty$, only the logarithmic terms diverge:

$$\sum_{j=1}^{j^*}\sum_{m=1}^{m_j}\frac{B_{j,m}}{2}\int_{k_{min}}^{k_{max}}\frac{2k+b_j}{(k^2+b_jk+c_j)^m}dk = \sum_{j=1}^{j^*}\frac{B_{j,m}}{2}\ln(k_{max}^2) + \vartheta = \sum_{j=1}^{j^*}B_{j,m}\ln(k_{max}) + \vartheta \tag{C10}$$

Finally, we have to analyze the last integrals in eq. C8. After the following linear transformation:

$$v = \frac{2k+b_j}{\sqrt{4c_j - b_j^2}} \tag{C11}$$

we can rewrite:

$$\left(C_{j,m} - \frac{B_{j,m}}{2}\right)\int_{k_{min}}^{k_{max}}\frac{dk}{(k^2+b_jk+c_j)^m} = \left(C_{j,m} - \frac{B_{j,m}}{2}\right)\left(c_j - \left(\frac{b_j}{2}\right)^2\right)^{1/2-m}\int_{\frac{2k_{min}+b_j}{\sqrt{4c_j-b_j^2}}}^{\frac{2k_{max}+b_j}{\sqrt{4c_j-b_j^2}}}\frac{1}{(v^2+1)^m}dv \tag{C12}$$

and, though it is not possible to write an explicit solution for the integrals of the form $\int 1/(v^2+1)^m$, integrating by parts we get:

$$\int\frac{1}{(v^2+1)^m}dv = \frac{v}{(2m-2)(v^2+1)^{m-1}} + \frac{2m-3}{2m-2}\int\frac{dv}{(v^2+1)^{m-1}} \tag{C13}$$

which allows to solve the integrals, yielding the appearance of rational and arctangent terms none of which diverges in the limit $k_{max}\to\infty$. Thus, only logarithmic terms from equations C7 and C10 contribute to the divergence of the initial limit of Eq. B3, that can be finally rewritten as follows:

$$\left|\lim_{k_{max}\to\infty}\int_{k_{min}}^{k_{max}}\frac{P(k)}{Q(k)}dk\right| = \ln(k_{max})\left|\sum_{i=1}^{i^*}A_{i,1} + \sum_{j=1}^{j^*}B_{j,m}\right| + \vartheta \tag{C14}$$

Thus, recalling that $|\vartheta| << \ln(k_{max})$ stands for finite terms, the only requisite for the limit to diverge is that:

$$\left(\sum_{i=1}^{i^*} A_{i,1} + \sum_{j=1}^{j^*} B_{j,m} \right) \neq 0 \tag{C15}$$

which is precisely the coefficient of the monomial of degree equal to $deg(Q) - 1$ in the numerator $P'(k) = P(k)/Q_o$, as can be easily shown after grouping the partial fractions in Eq. C5 into a single one. Therefore, we have demonstrated the initial statement: the condition for the integral in Eq. (C1) to diverge is that $deg(P') = deg(P) \geq deg(Q) - 1$.

Acknowledgments

The authors thank Maitane Gutierrez for assistance with design software to produce some of the figures. J. S was supported by MINECO through the FPU program. This work has been partially supported by MINECO through Grants FIS2011-25167; Comunidad de Aragón (Spain) through a grant to the group FENOL and by the EC FET-Proactive Projects PLEXMATH (grant 317614, to YM) and MULTIPLEX (grant 317532 to JS and SM).

[1] R.M. Anderson, R. M. May, and B. Anderson, *Infectious diseases of humans: Dynamics and Control* (Oxford University Press, Oxford, 1992).
[2] H. W. Hethcote, *The mathematics of infectious diseases*, SIAM Review **42** 599-653 (2000).
[3] D. J. Daley,and J. Gani, *Epidemic Modelling*, Cambridge University Press, UK, Cambridge (1999).
[4] J. D. Murray, *Mathematical Biology*, Springer-Verlag, Germany, Berlin (2002).
[5] J. Marro, and R. Dickman, *Nonequilibrium phase transitions in lattice models*, Cambridge University Press, Cambridge, (1999).
[6] L. J. S. Allen, *Some Discrete-Time SI, SIR, and SIS Epidemic Models*, Math. Biosciences **124** 83-105 (1994) .
[7] H. E. Stanley, *Introduction to Phase Transitions and Critical Phenomena*, Oxford University Press, Oxford (1987).
[8] H. W. Hethcote, *Qualitative analyses of communicable disease models*, Math. Biosci. **28** 335-356 (1976).
[9] R. Pastor-Satorras, and A. Vespignani, *Epidemic Spreading in Scale-Free Networks*, Phys. Rev. Lett. **86**, 3200-3203 (2001).
[10] R. Pastor-Satorras,and A. Vespignani, *Evolution and Structure of the Internet: a statistical physics approach*, Cambridge University Press, Cambridge (2004).
[11] A. L. LLoyd, and R. M. May, *How viruses spread among computers and people*, Science **292**, 1316-1317 (2001).
[12] S. Boccaletti, V. Latora, Y. Moreno, M. Chavez, and D. U. Hwang, *Complex Networks: Structure and Dynamics*. Phys. Rep. **424**, 175-308 (2006).
[13] S. N. Dorogovtsev, A. V. Goltsev, and J. F. F. Mendes, *Critical phenomena in complex networks*, Rev. Mod. Phys. **80**, 1275-1336 (2008).
[14] M. E. J. Newman, *The structure and function of complex networks*, SIAM Review **45**, 167-256 (2003).
[15] L. Hufnagel, D. Brockmann, and T. Geisel, *Forecast and control of epidemics in a globalized world*, Proc. Natl. Acad. Sci. USA **101**, 15124-15129 (2004).
[16] S. Eubank, H. Guclu, V. S. Anil-Kumar, M. V. Marathe, A. Srinivasan, Z. Toroczkai. N. Wang, *Modelling disease outbreaks in realistic urban social networks*, Nature **429**, 180-184 (2004).
[17] R. Pastor-Satorras, and A. Vespignani, *Epidemic dynamics and endemic states in complex networks*, Phys. Rev. E **63**, 066117 (2001).
[18] M. E. J. Newman, *The spread of epidemic disease on networks*, Phys. Rev. E **66**, 016128 (2002).
[19] Y. Moreno, R. Pastor-Satorras, and A. Vespignani, *Epidemic outbreaks in complex heterogeneous networks*, Eur. Phys. J. B **26**, 521-529 (2002).
[20] C. Castellano and R. Pastor-Satorras, *Thresholds for epidemic spreading in networks*, Phys. Rev. Lett., 105, 218701 (2010).
[21] M. Boguñá, and R. Pastor-Satorras, *Epidemic spreading in correlated complex networks*, Phys. Rev. E **66**, 047104 (2002).
[22] M. Barthélemy, A. Barrat, R. Pastor-Satorras, and A. Vespignani, *Velocity and hierarchical spread of epidemic outbreaks in scale-free networks*, Phys. Rev. Lett. **92**, 178701 (2004).
[23] M. Boguña, C. Castellano and R. Pastor-Satorras, *Langevin approach for the dynamics of the contact process on annealed scale-free networks*, Phys. Rev. E **79**, 036110 (2009).
[24] B. Guerra and J. Gómez-Gardeñes, *Annealed and Mean-field formulations of disease dynamics on static and adaptive networks*, Phys. Rev. E. **82**, 035101(R) (2010).
[25] S. Gómez, A. Arenas, J. Borge-Holthoefer, S. Meloni and Y. Moreno, *Discrete-time Markov chain approach to contact-based disease spreading in complex networks*, Europhys. Lett. **89**, 38009 (2010).
[26] J. Gómez-Gardeñes, V. Latora, Y. Moreno, and E. Profumo, *Spreading of sexually transmitted diseases in heterosexual populations*, Proc. Nat. Acad. Sci. USA **105**, 1399-1404 (2008).
[27] M. Tizzoni, P. Bajardi, C. Poletto, J.J Ramasco, D. Balcan, B. Gonalves, N. Perra, V. Colizza and A. Vespignani *Real-time numerical forecast of global epidemic spreading: case study of 2009 A/H1N1pdm*, BMC Medicine 2012, 10:165
[28] J. Sanz, M. Floría, and Y. Moreno, *Spreading of persistent infections in heterogeneous populations*, Phys. Rev. E **81**, 056108 (2010).
[29] V. Colizza, R. Pastor-Satorras, and A. Vespignani, *Reaction-diffusion processes and metapopulation models in heterogeneous networks*, Nature Physics **3**, 276-282 (2007) .

[30] S. Meloni, N. Perra, A. Arenas, S. Gomez, Y. Moreno, and A. Vespignani, *Modeling Human Mobility Responses to the Large-scale Spreading of Infectious Diseases*, Sci. Rep. **1**, 62 (2011).

[31] S. Meloni, A. Arenas, and Y. Moreno, *Traffic-driven epidemic spreading in finite-size scale-free networks*, Proc. Nat. Acad. Sci. USA **106**, 16897-16902 (2009).

[32] V. Belik, T. Geisel, and D. Brockmann, *Natural Human Mobility Patterns and Spatial Spread of Infectious Diseases*, Phys. Rev. X **1**, 011001 (2011).

[33] C. Poletto, S. Meloni, V. Colizza, Y. Moreno and A. Vespignani, *Host mobility drives pathogen competition in spatially structured populations*, PLoS comp. Biol. , **9(8)**, e1003169 (2013).

[34] F. Liljeros, C. R. Edling, L. A. N. Amaral, H. E. Stanley, and Y. Aberg, *The Web of Human Sexual Contacts*, Nature **411**, 907-908 (2001).

[35] Mossong J, Hens N, Jit M, Beutels P, Auranen K, et al. *Social Contacts and Mixing Patterns Relevant tothe Spread of Infectious Diseases*, PLoS Med **5(3) e74**. 0381-0391 (2008)

[36] B. Karrer, and M. E. J. Newman, *Competing epidemics on complex networks*, Phys, Rev. E **84**, 036106 (2011).

[37] Sebastian Funk and Vincent A. A. Jansen *Interacting epidemics on overlay networks*, Phys. Rev. E **81**, 036118 (2010).

[38] M.E.J. Newman. *Modeling the dynamical interaction between epidemics on overlay networks.*, Phys. Rev. E. **84**, 026105 (2011).

[39] V. Marceau, P.A. Noël, L. Hébert-Dufresne, A. Allard and L.J. Dub *Modeling the dynamical interaction between epidemics on overlay networks.*, Phys. Rev. E. **84**, 026105 (2011).

[40] J.A. Nelson, P. Ghazal and C.A. Wiley. *Role of opportunistic viral infections in AIDS.*, AIDS **vol. 4**, No. 1, 1-10 (1990).

[41] L.H. Kasper and D. Buzoni-Gatel *Some Opportunistic Parasitic Infections in AIDS: Candidiasis, Pneumocystosis, Cryptosporidiosis, Toxoplasmosis*, Parasitology Today **vol. 14**, no. 4, (1998).

[42] R.E. Chaisson, and N.A. Martinson *Tuberculosis in Africa – Combating an HIV-Driven Crisis*, New. Eng. J. Med. **358**, 11, 1089-1092, (2008).

[43] M. Nuño, Z. Feng, M. Martcheva, and C. Castillo-Chavez *Dynamics of Two-Strain Influenza with Isolation and Partial Cross-Immunity*, SIAM J. Appl. Math., **65(3)**, 964-982, (2006).

[44] P. Wang, M. C. Gonzlez, C. A. Hidalgo, and A.-L. Barabsi, *Understanding the Spreading Patterns of Mobile Phone Viruses*. Science **324**, 1071 (2009).

[45] P.-A. Noël, A. Allard, L. Hébert-Dufresne, V. Marceau, and L. J. Dubé, e-print arXiv:1102.0987.

[46] E.L. Corbett, C.J. Watt, N. Walker, D. Maher, B.G. Williams, M.C. Raviglione and C. Dye. *The global burden of tuberculosis. Global trends and interactions with the HIV epidemic*, Arch. Intern. Med. **vol. 163**, 1009-1021 (2003).

[47] C. Peikari, *Fighting fire with fire: designing a "good" computer virus.* InformIT, URL: http://www.informit.com/articles/article.aspx?p=337309, archived at http://www.webcitation.org/5kXXvHXfI on Oct 15, 2009.

[48] World Health Organisation tuberculosis database *http://www.who.int/tb/country/en/index.html*

[49] United Nations HIV datable UNADS *www.unaids.org*

[50] L.J. Abu-Raddad, et al. *Epidemiological benefits of more effective tuberculosis vaccines, drugs and diagnostics*, Prod. Nat. Acad. Sci., 106, 33, 13980-13985 (2010).

[51] M.C. Boily, C Lowndes and M Alary *The impact of HIV epidemic phases on the effectiveness of core group interventions: insights from mathematical models*, Sex Transm. Infect. 78, i78-i90 (2002).

[52] J.J. Moré *The Levemberg-Marquardt algorithm: implementation and theory.*, Numerical Analysis, Springer Berlin Heidelberg, 105-116 (1978).

[53] Au-Yeung et al. *Tuberculosis mortality in HIV-infected individuals: a cross-national systematic assessment*, Clin. Epidemiol. 3 21-29 (2011)